UCL

WORKING PAPERS SERIES

Paper 225 - Mar 21

The Socially-Distanced City: Speculation Through Simulation

The Socially-Distanced City
Speculation Through Simulation

Michael Batty

Centre for Advanced Spatial Analysis (CASA)
University College London, 90 Tottenham Court Road,
London W1T 4TJ

m.batty@ucl.ac.uk

March 8, 2021

Abstract

To explore the impact of the pandemic on the form and function of cities, we propose to simulate the forces of centralisation and decentralisation for different urban futures which we encapsulate in the spatial interaction patterns linking places of work to residence. Because the current pandemic has distorted locational patterns in current cities so radically, we first build a hypothetical city on square grid that we then proceed to lock down in terms of the percentage of the population no longer at their traditional places of work but working from home. We explore various pictures under different levels of lockdown showing how non-locked down activity responds to the changing urban landscape. We add some randomness to provide a greater degree of diversity and this partially breaks the symmetry of the idealised system. We then introduce different patterns of deterrence which imply different average trip lengths exploring a range of forms from highly centralised to decentralised. We illustrate how the system moves to different forms as we release the lockdown and let the system react to the continually changing urban landscape which produces a series of highly concentrated equilibria. This generates different patterns that we then perturb by adding a degree of randomness in the size of locations and we conclude by scaling the city from its 11x11 grid to one of 41x41 more illustrative of the diversity and degree of asymmetry in large cities like London. To progress this approach, we need to adapt our hypothetical model to real cities and continue such speculation through simulation.

Introduction: The Pandemic in World Cities

The world's first pandemic for just over a century has had an enormous impact on the landscape of cities. Patterns of movement and location have been dramatically disrupted as populations develop strategies for keeping apart from one another to avoid infection which is largely transmitted through direct or indirect human contact, through respiration or due to the virus being deposited on surfaces by those who have already been infected. Since pre-history, there have been a limited number of time-honoured strategies for keeping away from others based on social-distancing. Keeping at least 2 metres apart has been adopted by many during the last year, while working or studying from home amongst close family remote from one's usual workplace has been widely implemented, at times for up to at least 80 percent of the working and schools population. There has been a massive move to online activity, particularly education, shopping and entertainment and these have reinforced new patterns of remote human contact. There has been a pivotal change in movement, with transit falling to historic lows at less than 20 percent of its capacity in the largest cities, while many have taken to alternative transport such as walking and biking where possible (Florida, Rodríguez-Pose, and Storper, 2020). There has been a growth in car usage which is regarded as much safer than public transport and there is a clear increase in demand for country or ex-urban living with the suburbs becoming more popular than at any time during the last 40 years, reversing a slow but sure trend in returning to the central city.

When the pandemic began, there was a sense that life would return to normal which, in cities, would mean that traditional patterns of work, education and shopping would reassert themselves. There was however always a sense that we would move to a 'new normal' which would embrace some of these changes, particularly with respect to the online world (Batty, 2020a, b). In fact, with the emergence of a second, then perhaps a third wave of infection and the complex logistics of rolling out vaccines, it now appears that it will take much longer for the economy to rebound as we learn to live for some time with both the impacts of the disease and its continued containment. There is now quite wide speculation that the focus on ever growing central cities and the growth in central city populations and employment in the biggest cities will decline. Strategies for working from home at least for some part of the working week, online education and retailing, may become entrenched as the physical demand to visit traditional locations dissipates. In short ,cities may now begin to spread out again, thus resurrecting the suburban dream, while the emergence of automated personal transport will make safe, low cost, efficient, and comfortable travel more and more attractive.

In this paper, we will explore the impact of some of these changes, particularly those that deal with working from home and increasing preferences to travel further using suitably safe modes of transport which all impact on where people live and work, shop and go to school. We will begin by noting some anecdotal evidence concerning the use of transit, driving, walking, working from home and the use of retail facilities. These suggest the extent of the shift over the last twelve months in many cities around the world from data collected by Apple (2021) and Google (2021) in their mobility reports. These reveal a very substantial shift in where people work and shop and what modes of transport they continue to use to effect such interactions. We are not able to easily explore what will happen as regulations pertaining to restrictions on social contact ease in real cities other than through informed speculation but we are able to construct models that let us

simulate interactions in hypothetical cities where we can make assumptions about new locations and travel behaviours. The problem we face immediately in modelling these futures is that the baseline that we now have is an artificial one; existing travel patterns and locations have been distorted by what we refer to as 'lockdown' where those who can work from home are exhorted by government to do so while social distancing rules although not forbidding travel on public transport, have reduced their capacity very dramatically. To work with an 'artificial' city, we need to adjust the real city arbitrarily to this new regulated form where existing travel patterns are massively distorted, put on hold so-to-speak. We do not have detailed data on what this artificial form might be but because it is mandated, we can make very plausible assumptions as to what it looks like in hypothetical terms.

After our review of mobility trends, we will begin by constructing the hypothetical city on a square grid where we have a well-defined centre and a simple hierarchy of subcentres, not so dissimilar from the morphology of the city that we take as our exemplar, metropolitan London. Although highly monocentric at one level, it is also polycentric in that its subcentres are largely existing towns that have grown into its fabric. We construct this morphology on the simplest possible pattern of spatial interaction where simulate travel using the inverse square rule for the impact of distance on how far people travel. This is the default for the geometry that we construct and on top of this we impose a polycentric hierarchy which we then simulate using a standard transportation model which provides us with locations of employment, working population and trip movements symmetric around the centre. This we take as our working model for exploring artificial forms that result by assuming different proportions of workers who work from home. We start from no such working which is the normal picture, all the way to everyone working from home where employment has the same distribution as resident population with 'zero' distance travelled for the journey to work.

For our default pandemic city, we choose the form where some 80 percent of workers work at home and then simulate the trips consistent with this morphology using the standard transportation model. We use the simplest spatial interaction model based on the negative exponential function of distance to simulate this. From the lock down where 80% work at home, we then use the model to simulate changes in employment and residential locations using an unconstrained structure and this gives us a morphology that reflects what happens when workers are able to choose their new employment and residential locations consistent with their lockdown situation. This represents one of the many new normals and to show how we might make this more realistic, we introduce some random noise which changes the volume of activity at different locations. However we will not assume any further move to realism in this paper, but argue that the spatial interaction function embodies a set or behaviours which depend on how far or how near workers wish to be to their place of employment. For this we use a gamma-like function that enables us to simulate a range of morphologies from compact to suburban growth, thus providing a solution space within which many different forms of future city exist. To illustrate these potential change, we choose 9 different gamma functions defined by their parameters which in turn define a representative sample of cases in the solution space, revealing that under quite plausible assumptions, we can generate patterns of location and movement that are quite opposite to that which defines our starting point, or indeed the usual pattern prior to the pandemic. We then illustrate various long term equilibria

that result from releasing the lockdown with the urban landscape continually changing generating strongly focussed increases in activities towards the centre of the hypothetical grid. The extension of these ideas to real cities is an obvious next step but we will merely speculate on this by way of conclusions.

Profiles of Lock Down

The course of the pandemic almost everywhere has been clear and characteristic of successive waves of infection where the disease first spreads exponentially in time and space, the population then adopts various measures of social distancing which damp the wave, leading to a relaxation of controls which lead to yet another wave. In Britain for example, the first wave occurred between March and May 2020, then a relaxation occurred during the summer months with a second wave in the autumn, which was then suppressed by additional lockdowns. In turn these were relaxed as soon as there was any sign of the wave flattening. Almost immediately a third wave began, exacerbated by the winter months and this has led to a dramatic rise in mortalities, an order of magnitude more than during the first wave. In this period, the first vaccines were released and in Britain a massive vaccination programme began which looks as though it will suppress the virus and during 2021 will lead to some form of 'herd immunity'. There is now speculation that the virus may well become seasonal and that it will be one which will be present for some time to come.

The characteristic profiles of the pandemic that we will use here to build a model of social distancing for a hypothetical city are based on data that has been collected on different activities located at places where travel by different modes takes place. Data that is available that reveals social distancing, working from home, the use of different modes of transport such as driving (car), transit (in this case public transport by bus, rail or subway) and walking is not available from official censuses anywhere but it is available from the use of social media, particularly through map usage. Mobility Trends from Apple (2021) and Community Mobility Reports from Google (2021) provide excellent sources of data on a daily basis from the beginning of the pandemic in 2021 for many of the largest countries world-wide, data which is also disaggregated down to the case of regions, municipalities or below in the case of Google.

In Figure 1, we show the profiles for the United Kingdom and for Greater London from both these sources. The Apple data provides three sources of mobility data based on the numbers of persons driving, using transit, and walking which are measured with respect to a baseline of 100 and the percentage above or below this line (Figures 1a and 1b). The Google data measures the percentage displacement from a baseline measure at zero which gives numbers of persons visiting or using six different activity types, only one of which – transit stations usage – by location is comparable with the Apple data (Figures 1c and 1d). The other five are: Retail and Recreation, Workplaces, Residential, Grocery and Pharmacy, and Parks, of which we consider the first three to be key to our analysis of the factors influencing our model of the hypothetical city.

The profiles from Apple mirror those from Google for the most part with recovery after the first wave faster and more pronounced in the UK in the Apple mobility data, particularly transit, than the equivalent Google data. All these profiles show the waves of

infection and subsequent lockdowns quite clearly up until January 2021. In terms of transit data, the fall from the baseline is to about 25% below for the Apple data to 15% below for the Google data, both being more pronounced in London than elsewhere but nevertheless in all cases a precipitous drop. In London, this fall has remained at more than 50% throughout the last 12 months. Other modes of travel are rather different with driving falling to about 30% below but recovering to some 30% above by the time the second wave begins but then plunging again. Walking follows a similar trend. The Google reports reveal that the fall in retailing through the pandemic is substantial, down to 75% at the start of the period but never recovering to anything above 20% less than the baseline in the summer and now back again to something less than 70% below in London. The UK does a little better with similar profiles being less pronounced. In terms of working from home – residential – this is less easy to interpret as it assumes movement in an around the home and although this increases to something like 20% above the baselines, it cannot be compared to those at work which are much closer to the patterns of transit in both data sets. In London, those at work fall to 70% at the start of the pandemic and remain at no more than 40% throughout, now having fallen to about 60%.
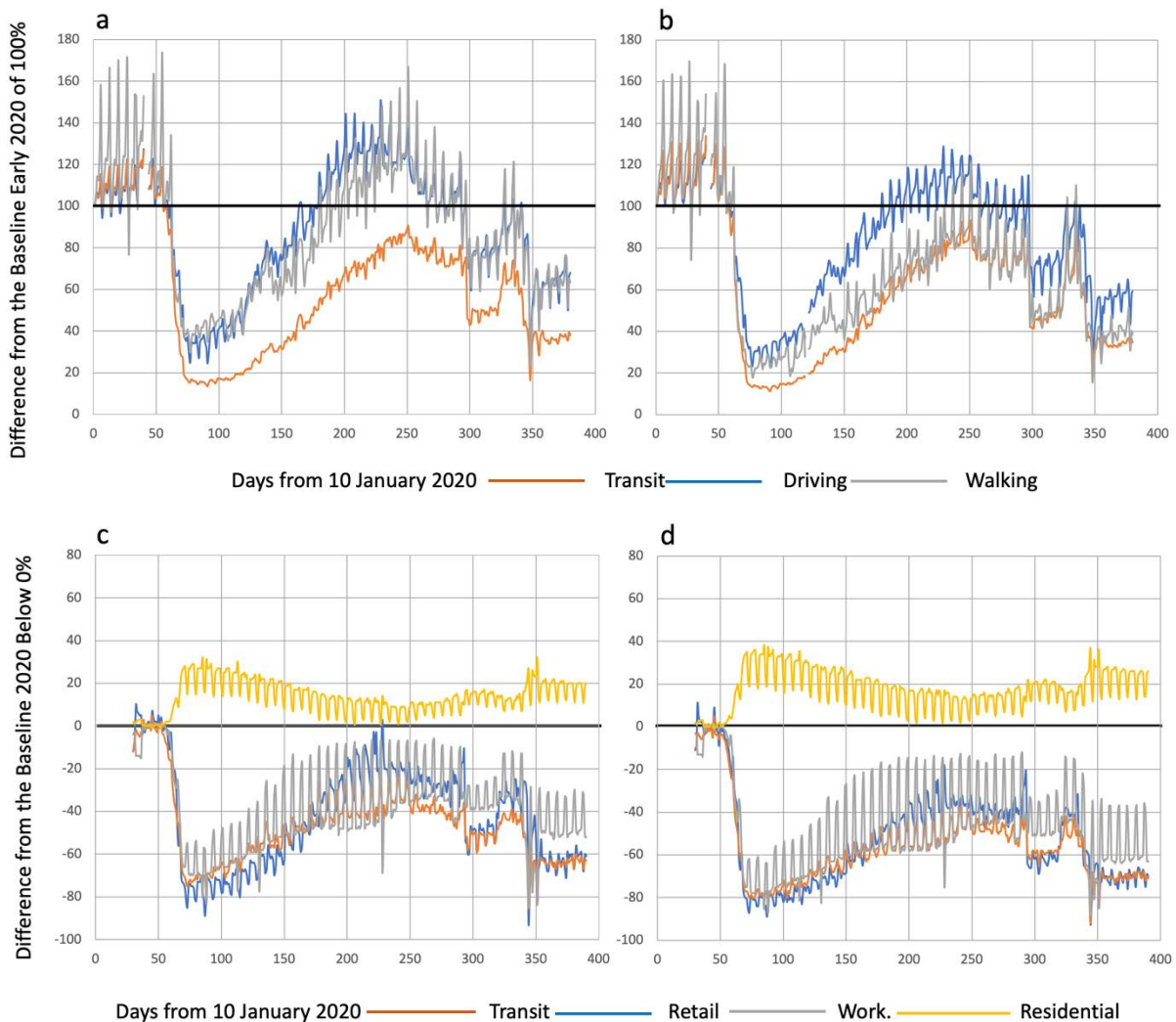

Figure 1: Measures of Mobility During 2020: From Apple for UK (a) and London (b), and From Google for UK (c) and London (d)

These profiles reveal considerable consistency in what the pandemic has meant for movement and location in cities and it is clear that during this last year in the largest cities those working from home have varied from a maximum of 85% to no more than 30% using Britain as exemplar. This is also reinforced by drops in mobility of the same order associated with transit but increases in driving in more suburban areas are a little larger than prior to the pandemic. We can thus assume that the percentage of those in work now working from home can be set as 80% although in our hypothetical city we will explore different percentages and shifts across the range of possibilities. We will also explore what it means for changes in the dominance of different modes of travel where public transport declines to levels that imply there are much longer trips made by those in work than prior to the pandemic. These will be reflected in the functions used to link home-based residential locations with work, origins with destinations, as we will refer to them in the simulations that follow.

Constructing the Hypothetical City

We define a city here as a set of N locations, $i, j = 1, 2, 3, …, N$, which form a square grid defined as an $n \times n = N$ set of cells. We assume these cells are square and adjacent and contiguous to one another but the system can be easily relaxed to take on any 2-dimensional geometry that is appropriate (Nugraha, et al. 2020). Each grid square i has a centroid defined by coordinates x_i, y_i which are associated with the grid as

$$x_i = [(i-1) \bmod n] + 1$$
$$y_i = int\left[\frac{i-1}{n}\right] + 1$$

$$\left.\right\} \quad . \tag{1}$$

The grid squares are arranged with the first ($i = 1$) located in the bottom left corner of the grid and the last ($i = N$) in the top right corner. The maximum distance d_{max} in the grid between these locations is defined as $d_{max} = [(x_1 - x_N)^2 + (y_1 - y_N)^2]^{½}$. This value is important because it defines the farthest distance anyone located on the grid can travel and as such in the simulations that follow, it is an upper bound on the mean trip length.

In fact, in the applications that follows, we fix $n = 11$ and this sets up the system as $n^2 = N = 121$ zones that we consider is manageable for exploring and visualising such a prototype. In fact at the outset, we need to make the system symmetric and this means that there is polarity about one location which is the central zone. This requires the number of zones on each side of the grid to be odd, that is, $n = 1, 3, 5, …$ which in turn means that the total number of zones N is also odd. Thus the central zone can be defined as $int[(n^2/2) + 1]$ and this is the most accessible point in the system with the sum of its distances to every other zone less than from any other point. This is an exceptionally important issue because what we will show in this paper is that this kind of symmetry is incredibly difficult to break. This is of course obvious as it is intrinsically part of our hypothetical cities such as those explored here but we also speculate it is as difficult to break in real cities for real cities which have similar polarity to our toy cities. We should also note the corollary of this accessibility which is the boundary effect that in small prototypes is likely to be significant. Many of these issues are likely to change qualitatively as we deal with ever larger grids which imply greater opportunities for

different morphologies due to their greater resolution. However our focus on the 11 x 11 grid would appear a useful starting point in that the system has enough variety to enable these centralising and decentralising effects on the central zone and the band of edge zones to be effectively captured.

We begin by constructing a default pattern of movements defined as $\{T_{ij}\}$ which measures the flows between all 121 zones where i defines the origin of the activity where people live and j defines the destination of the activity where people work. In this sense, then T_{ij} is the journey to work and we simulate this using the most basic gravitational model based on the inverse square law of distance which we state as

$$T_{ij} \propto 1/d_{ij}^2 \quad . \tag{2}$$

Note that the distances we use in this model are 'crow-fly' or 'airline' distances measured as $d_{ij} = [(x_i - x_j)^2 + (y_i - y_j)^2]^{1/2}$. The self-distance in each cell is set to 0.75, a little more than the nearest distance from the centroid to the edge of the cell, and less than the minimum distance to the nearest adjacent cell. We normalise this equation so that the total trips add to some predetermined total T and this means we can write the model as

$$T_{ij} = T \frac{d_{ij}^{-2}}{\sum_i \sum_j d_{ij}^{-2}} \qquad where \qquad \sum_i \sum_j T_{ij} = T \qquad . \tag{3}$$

To derive the numbers of residents at i called origin activity O_i and the number of workers at j called destination activity D_j, we sum equation (3) over j and i respectively

$$\sum_j T_{ij} = O_i \quad and \tag{4}$$

$$\sum_i T_{ij} = D_j \quad . \tag{5}$$

Now as the system is symmetric and so is the model, that is $d_{ij} = d_{ji}$, then $T_{ij} = T_{ji}$ and it is clear that the origin and destination activity are equal – that is as many workers work in each location as working population lives there, that is $O_i = D_i$.

This of course yields an entirely artificial situation which is never likely to be found in reality although various explorations of such models have been made to see how far from symmetry the real world of cities differs. Tobler (1976) has developed several variants based on such symmetry while variants of the model in equation (3) where explicit origin and destination variables differing from those observed are sometimes added as locational weights. Although we will not pursue this here, gravitational force encapsulated in the inverse square model in equation (3) has been considered an effect that should be factored out before any simulation takes place because it is an artifact of the system geometry. Coleman's (1964) method of residues exploits this idea and it has been used in simulating the effects of prior information on urban spatial interaction (Batty and March, 1976). Arguably some of these ideas would appear to be quite resonant with the disruptions in cities that we increasingly have to deal with (Couclelis, 2021).

We now have all the components in equations (1) to (5) to build the baseline for our hypothetical city system. Figure 2(a) presents the grid where it is clear that the number

of zones on each side of the square must be odd for there to be a central point coinciding with the grid. The origins and destinations $\{O_i\}, \{D_j\}$ are shown in Figures 2(c) and 2(d) where the locations are ordered by colour and size and we use this method throughout the paper but care must be used in interpretation for the scales are not uniform between the figures. Plotting the trip distributions are problematic as is widely known so what we have done in Figure 2(b) is plot the dominant direction of travel in terms of the average of the vectors to all destinations from each given origin which are defined as $\sum_j T_{ij}(x_i - x_j) = X_i$ and $\sum_j T_{ij}(y_i - y_j) = Y_i$. What we do is compute the direction associated with the coordinate pairs $dx_i = x_i - X_i$ and $dy_i = y_i - Y_i$ and these are shown as the tiny arrows in Figure 2(b). Were we to show their magnitudes as well, these highly symmetric flows would be confusing.

a   b

c   d
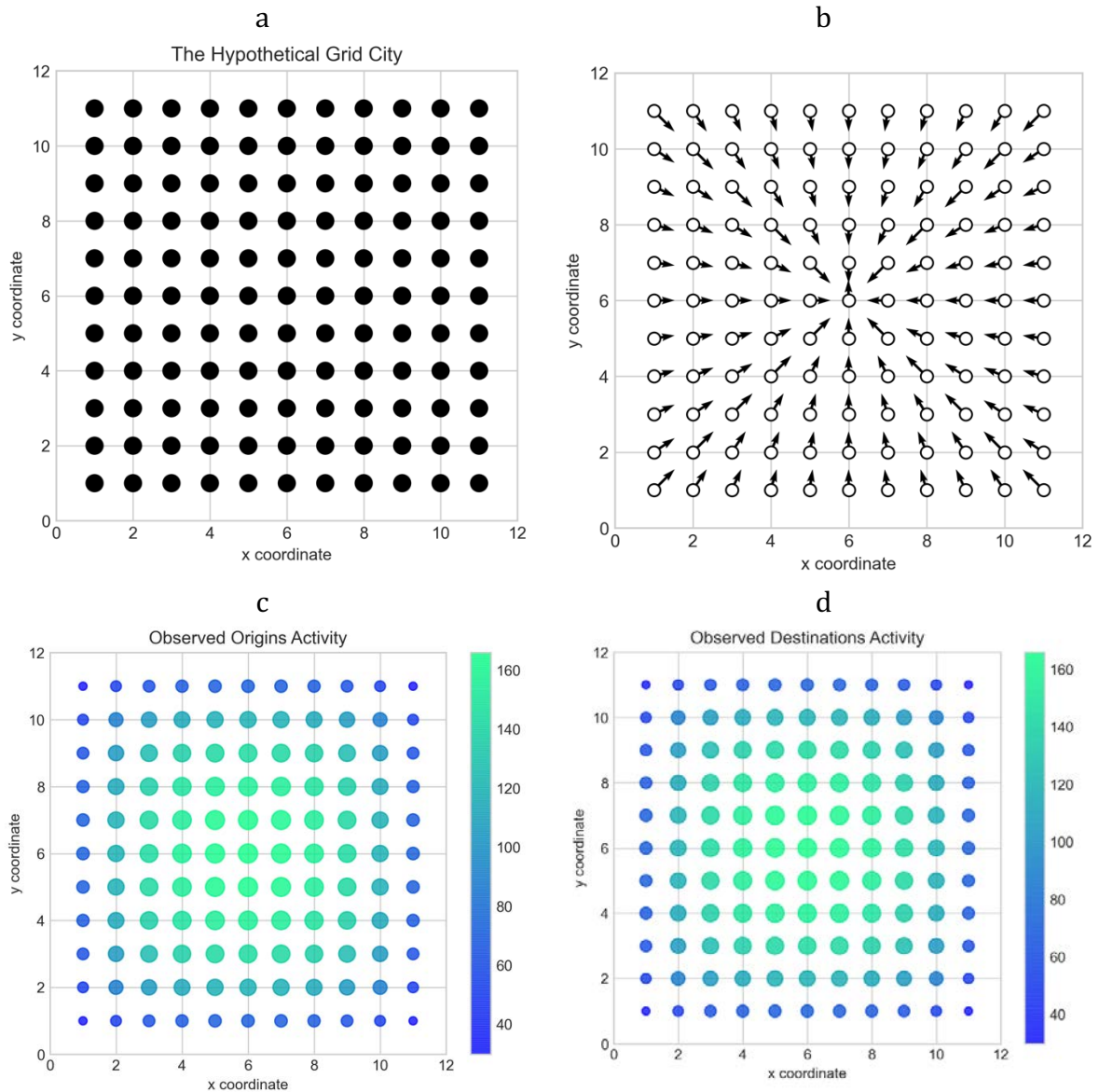
Figure 2: The Hypothetical Grid City

a) The 11 x 11 Grid b) The Dominant Vector Directions from Origins to Destinations c) Observed Origins by Size, and d) Observed Destinations by Size (which in this case, are the same as Origins)

This default landscape is far from what we observe in real cities. Within such urban fields, a hierarchy of different sized centres is usual while the single major centre is much larger

than the size of the central and origin and destination locations we have simulated in Figures 2(c) and (d). What we will do is impose a simple hierarchy of centres on this landscape by increasing the central destination D_{61} by 5 times, subcentres at $D_{37}, D_{41}, D_{81}, and D_{85}$ by 2 times, and $D_{13}, D_{21}, D_{101}, and D_{109}$ by 3 times. We keep the origin distribution the same as in Figure 2(c) and we show the new destination distribution in Figure 3(a). This is the default system we will work with in the next two sections. As we will continue to emphasise, it is extremely difficult to break symmetry in what is by default a symmetric hypothetical baseline (and the same is true of real city systems which are generically polar in their morphology). But we are able to show how this is done in Figure 3 where we show a new distribution of origins based on $T_{ij} \propto 1/d_{ij}^{12}$, in terms of destinations, the central location as $D_{61} = 0$, and the edge cities around the outer band of boundary zones as 2 times the original destinations with the next inner band as 3 times the original destinations in Figure 2(c). We show these new data in Figure 3(b) and (c) and we then show that flow directions in Figure 3(d) where there is very clear evidence of symmetry breaking.
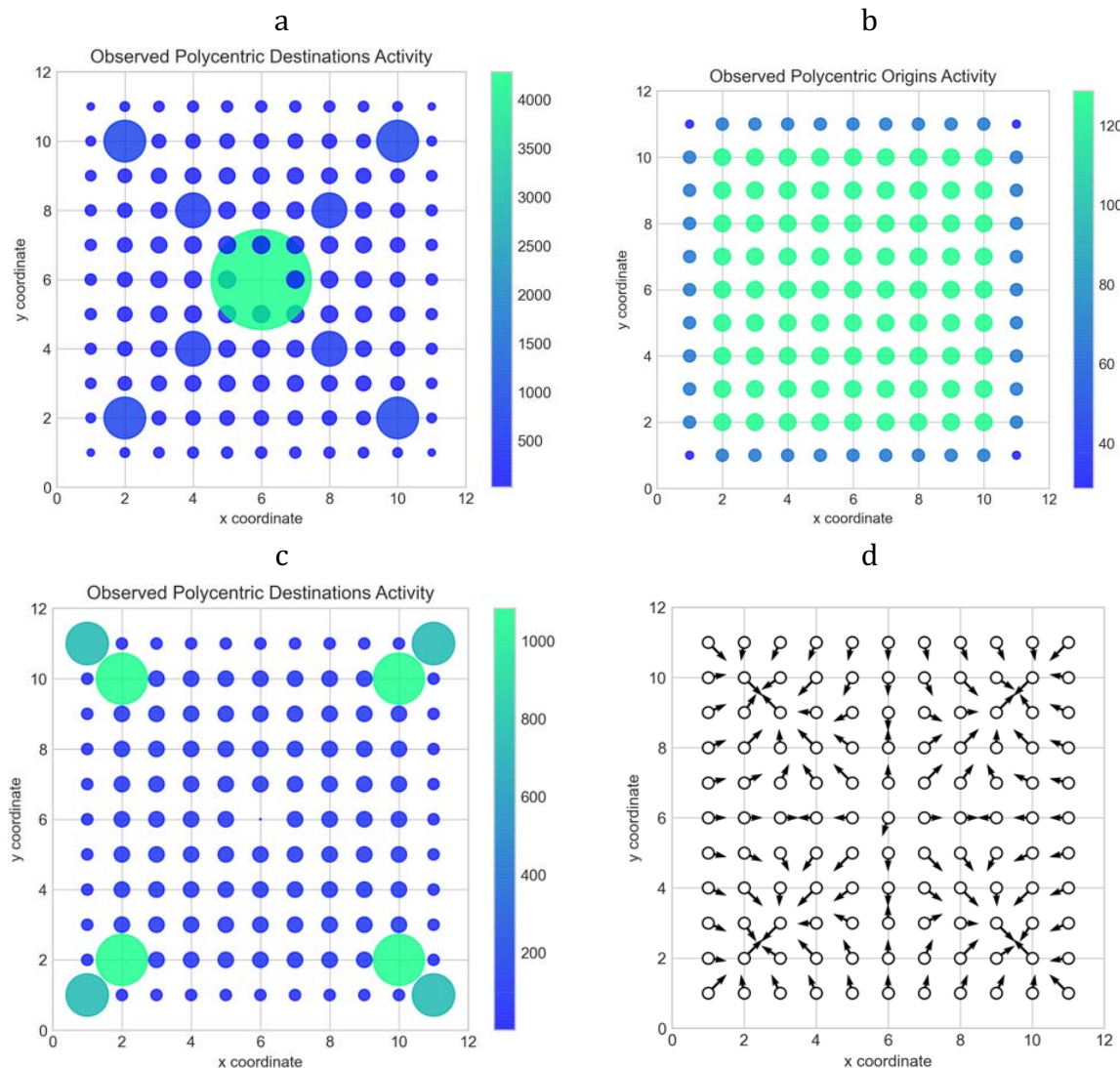

Figure 3: The Hypothetical City with Two Polycentric Forms Imposed on the Baseline

a) The Imposed Hierarchical Destination Locations b) Breaking Symmetry with a New Distribution of Origins c) Location of Edge Destination Polycentres d) Symmetry Broken by the New Origins and Edge Destinations

The last thing we need to do to prepare our baseline for changes imposed by social distancing and the penchant to work from home during the pandemic. We will then provide a full simulation of the city form we have manufactured. First however we need to note that the average mean trip length for the first baseline is defined as

$$\bar{C} = \sum_i \sum_j T_{ij} d_{ij} / \sum_i \sum_j T_{ij} \qquad . \qquad (6)$$

For the 121 zone system, this value $\bar{C}$ is 2.516 compared to a uniform distribution across the grid where the average distance is 7.071. The maximum distance across the system is twice this at 14.142. We are now in a position to fill in the detail for the polycentric baseline which is the system based on origins in Figure 2(c) and the destinations based on Figure 3(a). What we now do to construct the trip distribution associated with this morphology is to develop a constrained model which meets the origin and destination constraints associated with this baseline. To do this, we use the standard doubly constrained model with a negative exponential function of distance. We state this as

$$T_{ij} = A_i O_i B_j D_J \exp\left(-\beta d_{ij}\right) \qquad , \qquad (7)$$

where the scaling constants A_i and B_j are chosen so that the model is consistent with the origin and destination constraints

$$\sum_j T_{ij} = O_i \ \text{ and. } \ \sum_i T_{ij} = D_j \qquad . \qquad (8)$$

These constants which are also called competition terms or balancing factors have to be solved iteratively from

$$\left.\begin{array}{l} A_i = \dfrac{1}{\sum_j B_j D_J \exp\left(-\beta d_{ij}\right)} \\[2em] B_j = \dfrac{1}{\sum_i A_i O_i \exp\left(-\beta d_{ij}\right)} \end{array}\right\} \qquad . \qquad (9)$$

We choose a value for $\beta = 1/\bar{C}$ which is 0.397 and this then generates a mean trip length for the model in equations (7) to (9) as $\bar{C} = 3.388$. This would appear to be a reasonable value for a system with the dimensions of our default hypothetical city.

When we examine the direction of travel from origins to destinations in these baseline models, the symmetry of the original structure is maintained in all cases and as we will see, this is the case for most of the examples in this paper. To really break symmetry we probably need to move to much bigger systems where there are more opportunities to provide very different locational patterns. At the same time, we need to introduce considerable noise, that is, much greater heterogeneity into the system. This must await further work for we now need to explore what happens to this toy city under different levels of social distancing, and changes in travel behaviour.

The Socially-Distanced Locked Down City

Once the pandemic began in earnest in March 2020, amongst the many changes in our behaviour, the rapid movement to working from home for up to 80% of the working

population, the reduction in the use of public transport and the slow but significant change in behaviours which have pushed people to live further from their traditional places of work, can all be introduced into our hypothetical city through changes to the spatial interaction model. In this section, we will move people arbitrarily from work to home and then examine the pattern of how origins and destinations adjust to these kinds of disturbance. We define the proportion of the population working as usual in their places of work (destinations) as $\lambda, 0 \leq \lambda \leq 1$, and the proportion of those living and working at home as $1 - \lambda$. In essence, there is no change in terms of where people live but in the different scenarios based on a varying proportion of those working from home, workers are assigned from their job locations to their home locations according to the system-wide proportion $1 - \lambda$ of those working from home. We do not vary this with respect to locations although it is does vary a little in reality with respect to the proportion of workers defined by the UK government as key workers (Farquharson, Rasul, and Sibieta, 2020). We thereby assume that the proportion is stable over all workers and locations in our toy city and with this assumption, we are able to produce new scenarios based on a simple scaling and reallocation of jobs to home locations.

A new distribution of trips $\hat{T}_{ij}$ which differs from the original modelled distribution T_{ij} due to this reallocation can be defined as

$$\hat{T}_{ij} = W_{ij} + H_{ij} \tag{10}$$

which is split into those workers who continue to live and work in the same manner as previously $W_{ij} = \lambda T_{ij}$ and those who now live and work exclusively from home H_{ij}. If we sum these trips over destinations which are job locations, these must equal the numbers of workers living in origins O_i which does not change. Then

$$O_i = \sum_j \hat{T}_{ij} = \lambda \sum_j T_{ij} + \sum_j H_{ij} \quad , \tag{11}$$

from which it is clear that

$$\sum_j H_{ij} = (1 - \lambda)O_i \quad . \tag{12}$$

The constraint on where people live is the same as in the basic model, that is

$$O_i = \lambda O_i + (1 - \lambda)O_i \quad . \tag{13}$$

The distribution of jobs at destinations D_j does however change as we need to reallocate a proportion of jobs associated with the existing locations so that workers can work from home. This means that there are no longer any of these workers who travel to work and the matrix $[H_{ij}]$ must reflect this., that is $H_{ij} = 0, i \neq j$, while all the jobs associated with any residential location i through the trips T_{ij} are reassigned to i as

$$H_{ij} = H_{ii} = (1 - \lambda) \sum_k T_{ik}, \quad i = j \quad . \tag{14}$$

It is easy to show that

$$H_{ii} = (1 - \lambda)D_i, \quad i = j \quad , \tag{15}$$

and the total destinations activity is thus

$$\widehat{D}_j = \lambda D_j + (1 - \lambda)O_j \qquad . \qquad \qquad (16)$$

Note that our scenarios are based on changes to trips and destination activities $\widehat{T}_{ij}$ and $\widehat{D}_j$ that depend on the proportion of workers λ working from home, and it is this parameter that we will vary from $\lambda = 0$ which is everybody working from home to $\lambda = 1$ which is the polycentric city that is our starting point.


a

b

c

d
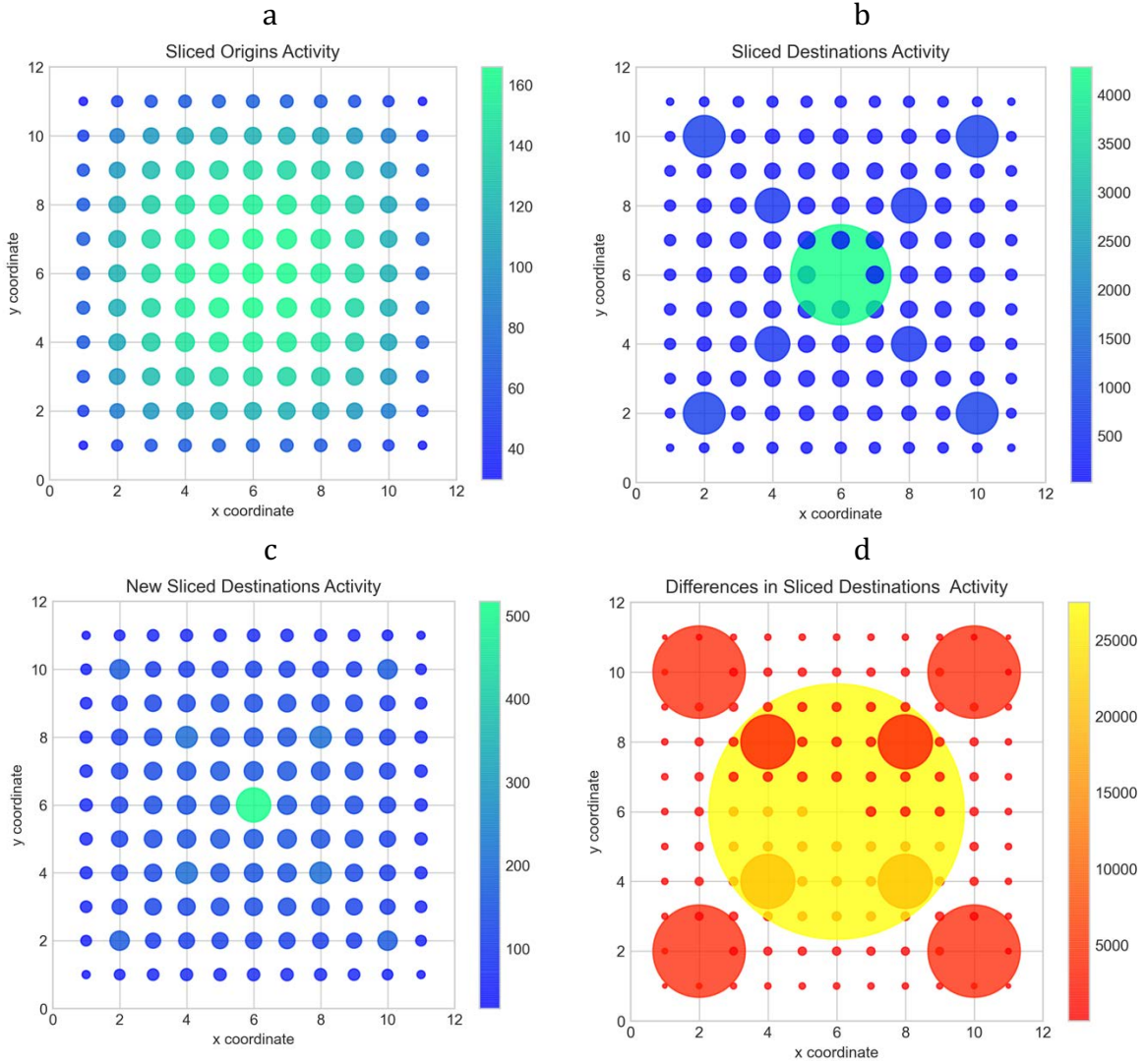
Figure 4: The Hypothetical Polycentric City with $1 - \lambda = 0.8$ Working From Home

a) Origin Locations b) Polycentric Destination Locations c) Destination Locations for Those Still Working at Original Workplaces, and d) Absolute Differences Between Origins and New Sliced Destinations $\psi|O_i - D_i|$

We have explored the range of possible regimes based on working from home which involve changing the distributions of workers at their place of work $\widehat{D}_j$ given by equation (17). The origin distribution remains the same as pictured in Figure 2(c) for any value of λ and beginning with $\lambda = 0$, this implies that, everyone works from home and that the distribution of new workplaces is the same as the distribution where people reside. As we increase λ, the polycentric pattern of workplaces begins to reveal itself and as α

approaches 1, the polycentric pattern that we see in Figure 3(a) appears. We cannot show this here, but as we change λ continuously, we animate the destination location patterns showing how the residential pattern which dominates the complete working from home scenario transforms the residential pattern into the workplaces pattern. We will show only one sample from this transformation here, that based on the situation where 80% of workers work from home (with 20% following traditional spatial interactions). This is consistent with our data that we introduced as background information in the first section of this paper and we show the simulations in Figure 4, where we also show the difference between the original polycentric distribution of workers and the new distribution based on $\lambda = 0.2$.

There are many ways of measuring the differences in morphology which are occasioned by the range of what we loosely refer to as slicing the workplace into those who work from home and those who remain in their traditional workplace. When everyone works from home, the mean trip length $\bar{C}$ is the lowest it can be which is the smallest distance in a cell set at 0.75. As the proportion working from home decreases, then this trip length increases back to the level specified in the original data $\bar{C} = 3.388$. There are several other measures that show this changing morphology for workplaces in particular entropy measures of which the basic Shannon entropy can be computed for destination distributions as

$$
\left.
\begin{aligned}
H(D) &= -\sum_j p(D)_j \, log \, p(D)_j \\
H(\widehat{D}) &= -\sum_j p(\widehat{D})_j \, log \, p(\widehat{D})_j
\end{aligned}
\right\} \tag{17}
$$

where $p(D)_j$ is the probability of the cell i being the original value D_j and $p(\widehat{D})_j$ is the new value for the sliced destination distribution based on $\widehat{D}_j$. In fact these entropy values do differ as λ changes but not by very much, changing only by about 2 percent over the range. This is due to the fact that although there might appear to be considerable differences between the two distributions especially when everyone works at home, the grid is too small and the variations in D_j and $\widehat{D}_j$ not big enough for these measures to be particularly good discriminators. A better measure appears to be the Kullback information statistic defined as

$$
I\left(\frac{\widehat{D}}{D}\right) = -\sum_j p(\widehat{D})_j \, log \left\{\frac{p(\widehat{D})_j}{p(D)_j}\right\} \quad , \tag{18}
$$

which varies from 0.5 to zero indicating the biggest changes take place when the numbers of people working from home first starts. In fact more intuitively obvious measures of change are based on actual differences between these variables in terms of their size and for the destinations distributions we can compute such differences as being based on $\sum_j |D_j - \widehat{D}_j|$. We will plot a much wider range of these measures a little later when we examine differences in travel behaviour patterns. The different range of patterns does not reveal any real spreading out of the hypothetical city other than in the removal of the strong polycentric structure when people begin to work from home. When we look at the dominant movements in the system using the directional vector fields this simply indicates that the original symmetry in Figure 2(b) is maintained. To break this symmetry, we have explored the extent to which introducing variety into the initial origin

and destination distributions through a measure of random noise would enable this and we will explore these in the next section.

Simulating Lock Down and Diversifying the Urban Landscape

We will take the lockdown in the polycentric city based on some 80% of people working from home and use its unchanged origin and new destination distributions as inputs to the unconstrained gravitational model that will let us recompute the numbers of persons in origins and destinations. We argue that a simulation like this is an emergent structure from a situation where people get used to working from home but when the lockdown is released and they consider returning to work, then the pattern of where such work is likely to be and where they wish to live is different from that prior to and then under lockdown. In short we take the sliced origins and new sliced destinations in Figure 4 and use these as inputs to an unconstrained gravitational model which predicts new patterns of location and interaction. The model we use is based on a variant of that in equation (7) given as

$$\hat{T}_{ij} = KO_i D_j \exp\left(-\beta d_{ij}\right) \quad where \quad \sum_i \sum_j T_{ij} = T \tag{19}$$

and K is the scaling constant that ensures that the flows add to T. The model is then used to predict a new distribution of origins and destinations which are

$$\left.\begin{array}{l} \hat{O}_i = \sum_j \hat{T}_{ij} \\[2mm] \hat{D}_j = \sum_i \hat{T}_{ij} \end{array}\right\} \quad , \tag{20}$$

In short, we are now simulating a new equilibrium from the socially-distanced artificial lockdown and the full results of this can be seen in Figure 5.

In fact the origin activity where the working population resides is more polarised than the original distribution while the polycentric form for destination activity is slowly returning. In fact this shows that the centralising forces implicit in the urban structure that we have adopted are extremely strong and this is revealed by the difference maps in Figures 5(c) and (f). A word of caution here in interpreting these diagrams. The differences are taken as absolute values and do not indicate activity less than that observed. In short, the inner zones for both origins and destinations show locations where new activity is greater whereas the outer zones show where activity is less. These figures need to be read with Figures 5(a) & (b) for origins and (d) & (e) for destinations. To attempt to break symmetry, we have developed the same sort of simulation but his time we have introduced a very substantial amount of noise for both origin and destination distributions. What we have done is to scale origins O_i and lockdown destinations $\hat{D}_j$ by $[1 \pm rand(\ )]$ and this enables activities to increase up to double their size or reduce to almost zero. After this randomisation, the activities are rescaled to reflect the total activity T in the system. We have rerun the model in equations (19) and (20) for a first iteration and then for five more using the outputs from the unconstrained model on each iteration to provide inputs to the next. Five iterations really does indicate the long term structural equilibrium of the system and it appears to be heading to a

situation where everything is concentrated at the core with respect to both origin and destinations activity. Figure 6 reveals the picture after the first and the fifth iterations.
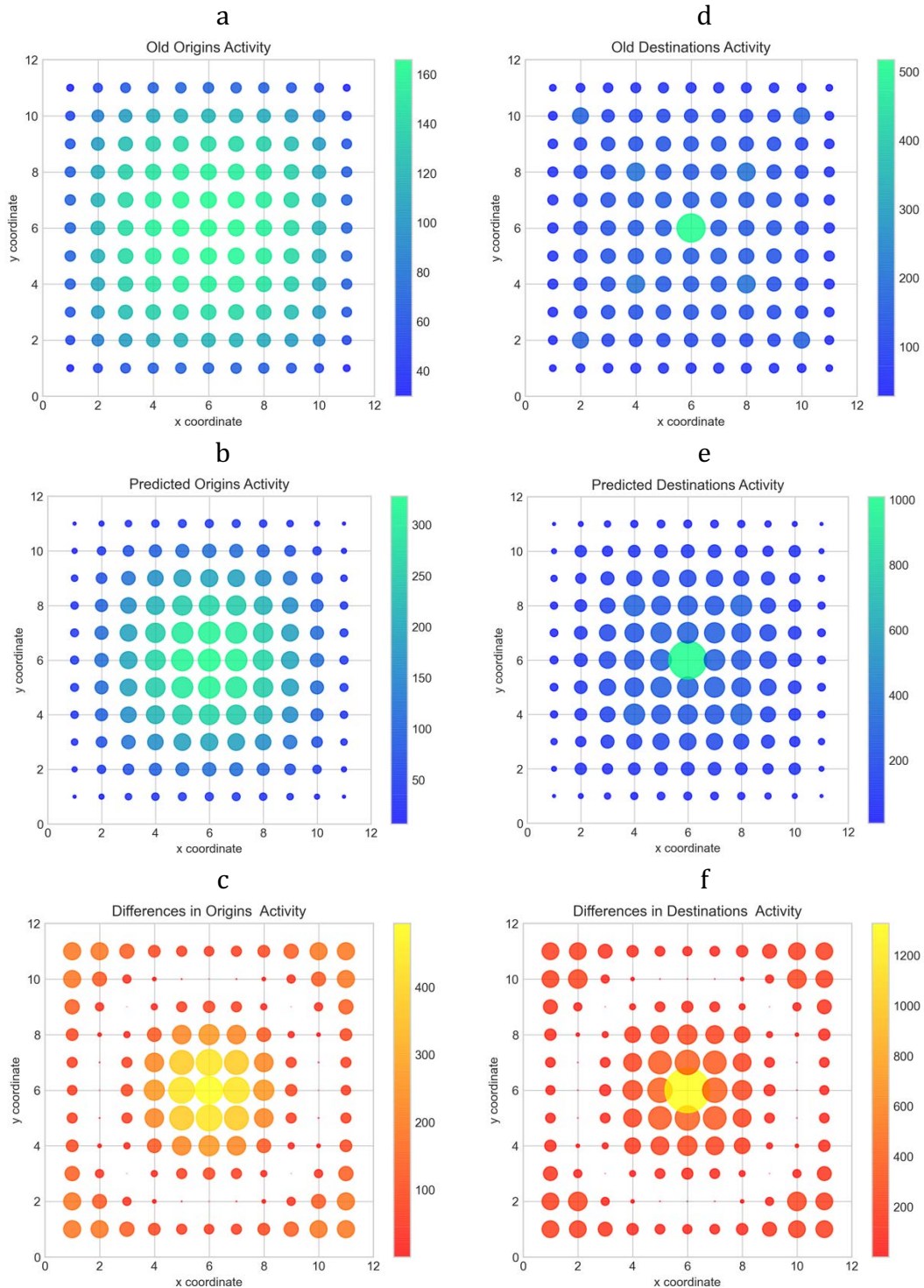

Figure 5: Unconstrained Simulations of Origins and Destinations from the Locked Down Based on 0.8 *Working at Home*

a) Working at Home Origins b) Predicted Origins c) Scaled Differences based on $|O_i - \widehat{O}_i|$ d) Still at Work Destinations e) Predicted Work Destinations f) Scaled Differences based on $|D_j - \widehat{D}_j|$,

first iteration a   d

outputs from the first iteration b   e

a long term equilibrium c   f
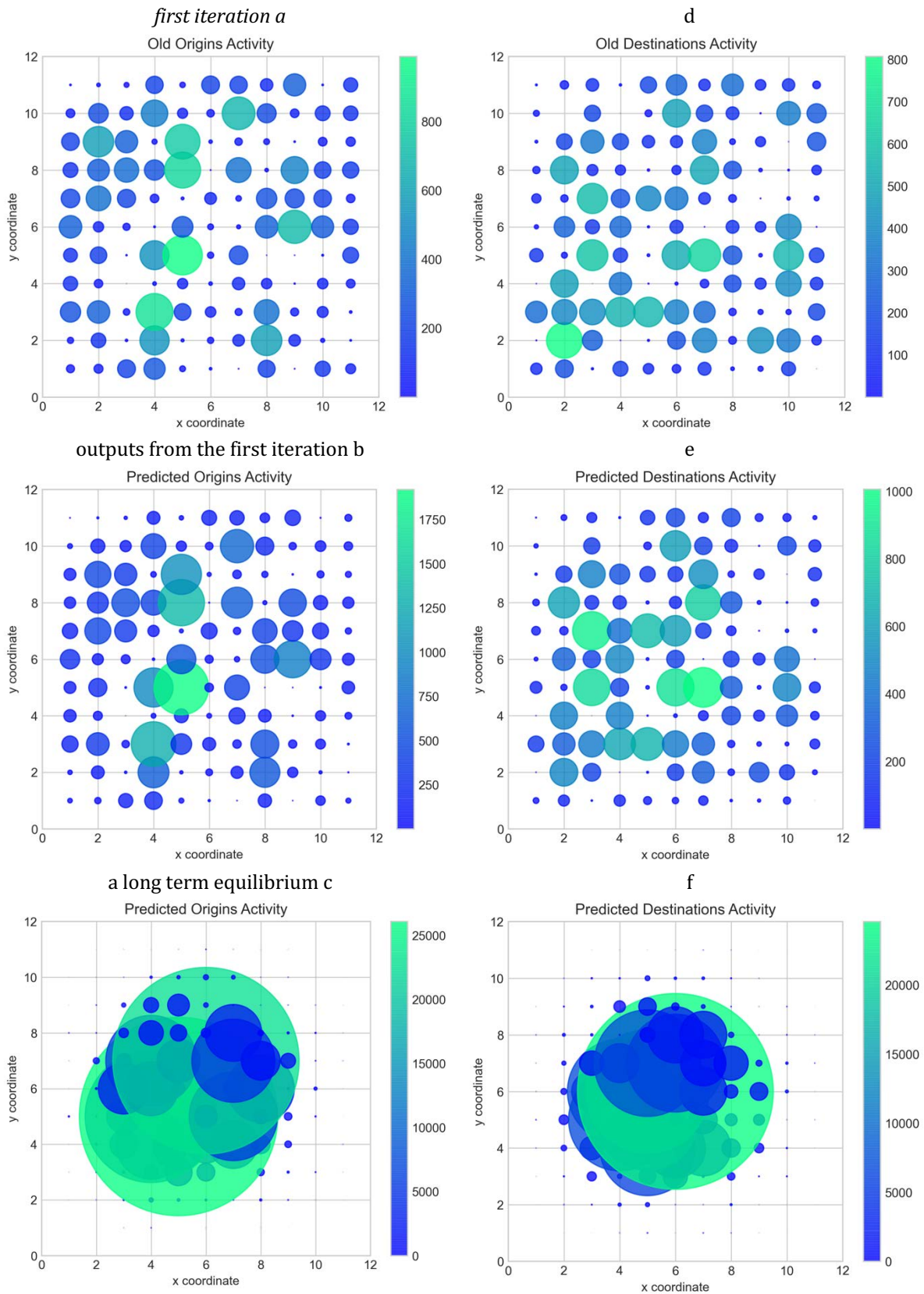
Figure 6: Iterative Solution of the Transition to Equilibrium from the Randomised Lockdown Distribution of Residents and Workers, at Origins and Destinations Respectively

There is still no evidence of symmetry breaking in the landscapes we reveal in Figure 6. In fact this is quite the reverse with symmetry being massively reinforced. We have run the model for many more iterations (>50) and what happens is that all the activity with respect to both origins and destinations ends up at the central zone. To explore how we might simulate a more diverse city, one in which it is easier to detect changes in the degree to which activities concentrate or disperse, we need to explore how we can change travel behaviour in the model and the city system. To do this will define a parameter space of travel behaviour and indicate how we might articulate it in the effort to find both general trends as well as particularly interesting morphologies

Searching the Parameter Space of Different Travel Behaviours

The first pattern of movement which we used to build the landscape of our toy city was based on the simplest gravitational force, the inverse square law, which is based on the assumption that movement varies inversely with distance from the point at which that movement begins. This is sometimes called the 'First Law of Geography' or sometimes Tobler's Law after Waldo Tobler's (1970) almost throwaway remark in one of his early papers (Sui, 2004). We used the function $T_{ij} \propto d_{ij}^{-2}$ to construct the landscape of origins and destinations but then on top of this, we layered an arbitrary hierarchy of workplaces which we then normalised using a much more widely accepted negative exponential function $\exp\left(-\beta d_{ij}\right)$ used to generate a consistent pattern of movement as reflected in equations (7) to (9). In fact neither of these inverse distance functions is entirely suitable. The inverse square law is undefined at zero origins and predicts far too many interactions at small distances while the negative exponential function is also unable to deal with small distances particularly where there are mild preferences to live some distance away from work, for example, something that we need to exaggerate in structuring our model to deal with social distancing.

Accordingly we need a function with much greater flexibility and one which has found some use in spatial interaction is the gamma function, or rather a gamma-like function that combines both inverse power and negative exponential effects. We can state this function as

$$T_{ij} \propto d_{ij}^{\alpha-1} \exp\left(-\beta d_{ij}\right) \qquad\qquad (21)$$

where the parameters α and β control the friction of distance for the power and exponential functions respectively. When $\alpha = 1$, then the power function collapses and the function reverts to the negative exponential. When $\beta = 0$, the negative exponential collapses and the model reverts to the power law. When $\alpha > 1$, the power law no longer acts as a deterrent effect but as an attractor but this is moderated by the negative exponential which acts as the deterrent. We show nine different varieties of this effect in Figure 7, these being the functions that we will use in the sample simulations that follow. In fact we illustrate these in the Appendix and simply pick out the major characteristics of these simulations here in the main text. These are not in any particular order and we will briefly comment on them as these contain various scenarios that define the parameter space that we will explore below. However, it is worth noting that this gamma function was first proposed by Tanner (1961) to handle small distance effects in trip

distribution models but in generalising the gravity model, it has been used several times since Tanner's original suggestion (see for example, Cochrane, 1975).
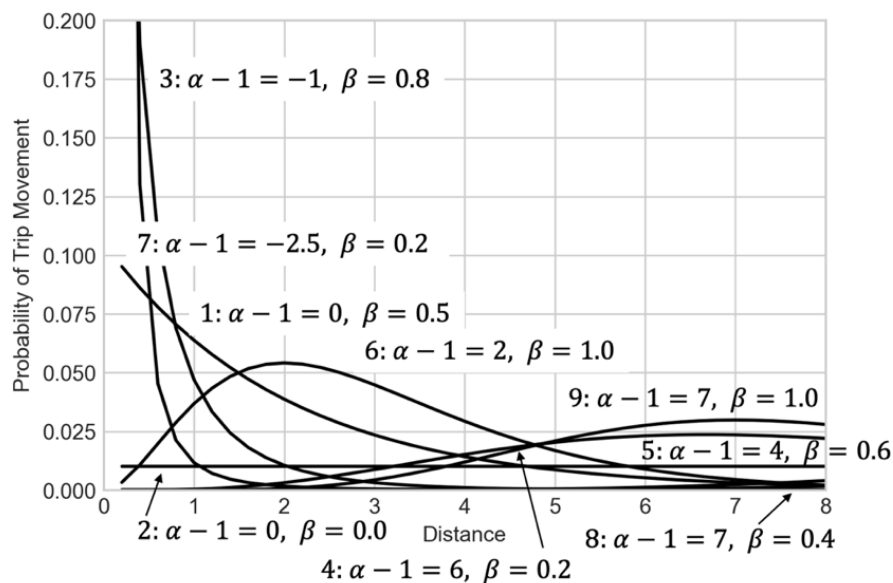

Figure 7: Probabilities of Trip-Making with Respect to Distance Under Different Combinations of the Two Parameter Gamma Distribution $\alpha - 1$ and β

We have taken as our starting point the locked down city where 80% of the working population work from home and we first simulate a baseline case from the distributions shown in Figure 4. This baseline is produced from the pure negative exponential distribution based on the unconstrained gravity model in equation (19) defined by scenario 1 where $\alpha - 1 = 0$ and $\beta = 0.5$. This generates a pattern where the origins and destinations are more polarised around the centre than the pattern based on the default of 80% working from home. When we lower the β to 0 the pattern is less polarised and when we move back to $\alpha - 1 = -1$ and $\beta = 0.8$, the pattern in the first scenario begins to reassert itself.

We then switch the parameters to $\alpha - 1 = 6$ and $\beta = 0.2$ and generate a city which is blown to its edges with origins and destinations increasing inexorably from its centre to its edge. This is clearly generated by the increase in $\alpha - 1$ which shows a distribution function which is the opposite of the inverse deterrence function. This implies that people wish to live well away from the centre in that the central core is increasingly unattractive as one moves from home and work. As we change $\alpha - 1$ and β to 4 and 0.6 and then to 2 and 1.0, the origins and destinations become less pronounced but begin to reinforce the traditional patterns focussed on the central zone. If we fixe these at -2.5 and 0.2, we reinforce the monocentric pattern once again. If we then move to 7 and 0.4, we reinforce the edge effects and both origins and destinations decentralise. When we increase β to 1.0 and raise $\alpha - 1$ to 7, then the tension between these two elements in the function with the power law component pushing the system to decentralise and the exponential to centralise, leads to a more muted pattern similar to the original lockdown in Figure 4.
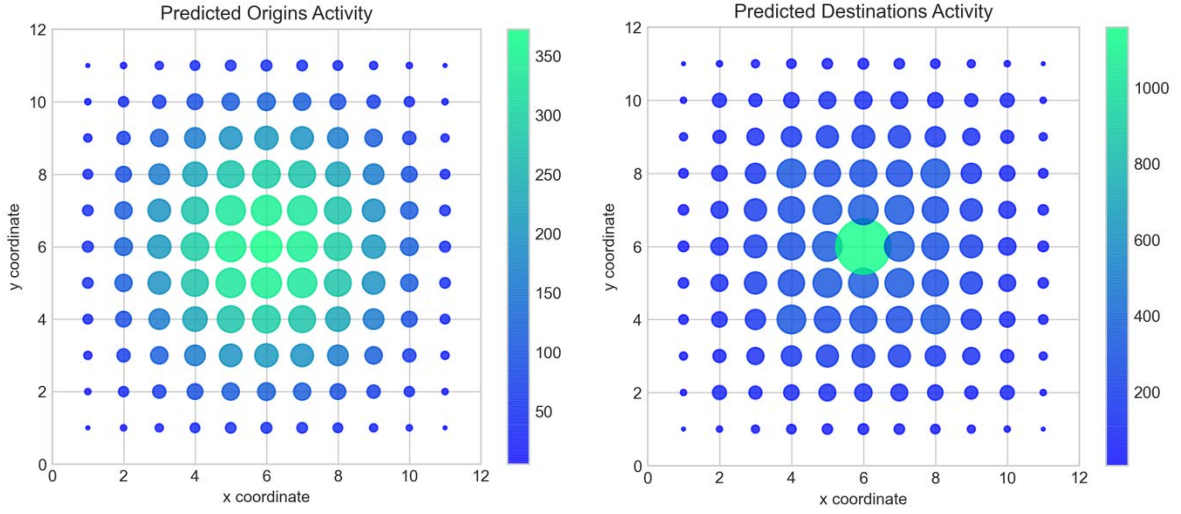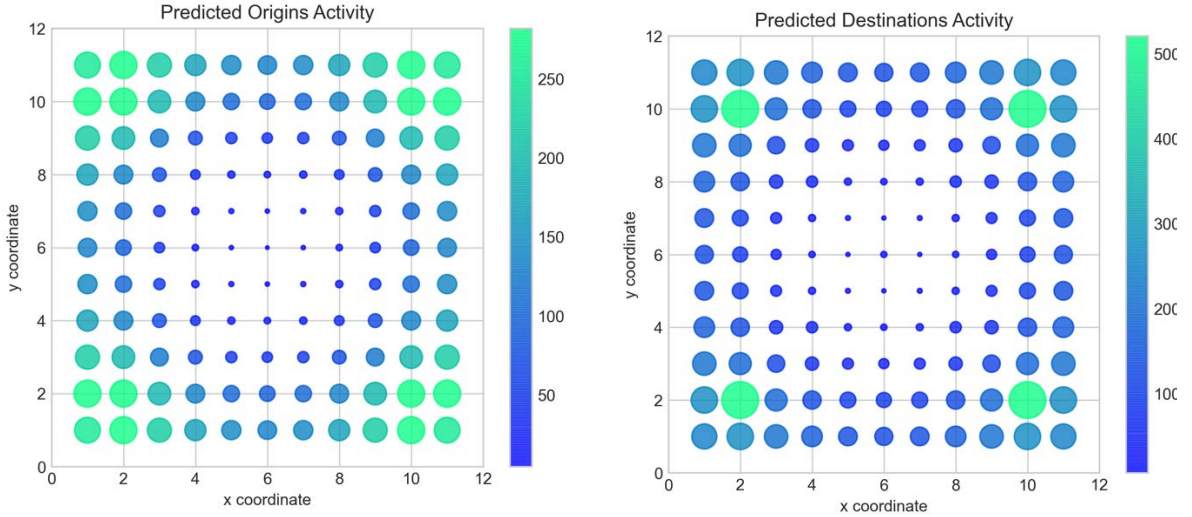
Figure 8: Scenarios 6 and 8 Showing Their Equilibria in Terms of Predicted Origins and Destinations Using Different Travel Behaviour Functions

We will illustrate the two extreme examples in this sample of 9 different travel behaviours and we show these in Figure 8. These are two from the 9 that we show in their entirety in the Appendix. In fact we have consistently and comprehensively explored all possible scenarios in the solution space for the range of parameters from $\alpha - 1 = -2\ to\ 7$ and $\beta = 0.0\ to\ 1.0$ which are shown in Figure 9 where the mean trip lengths associated with the gamma distribution, $\bar{C} = \sum_i \sum_j T_{ij} d_{ij} / \sum_i \sum_j T_{ij}$ and $\hat{C} = \sum_i \sum_j T_{ij} log\ d_{ij} / \sum_i \sum_j T_{ij}$ indicate that these increase more or less linearly with $\alpha - 1$ and β. These are shown in Figures 9(a) and 9(b) respectively. When we plot the differences between origins from those that are input to those output $\sum_i |O_i - \hat{O}_i| / N - 1$ and the same for destinations $\sum_j |D_j - \hat{D}_j| / N - 1$ these two decrease linearly and are shown in Figures 9(c) and 9(d) while in Figure 9(e) we show the mean trip length less 3.388 which is the value of the existing simulation less the value for the initial locked down model. What we are really searching for in this solution space are any nonlinearities that suggest that there are unique points where a best combination of two parameters can be identified. For

example, from our original data, we might identify values of $\bar{C}$ and $\hat{C}$ that define a unique combination of parameter values. From the initial lockdown, we calculate $\bar{C} = 3.38$ and $\hat{C} = 1.05$ identifying a unique position in Figures 9a & b which are of course hypothetical.
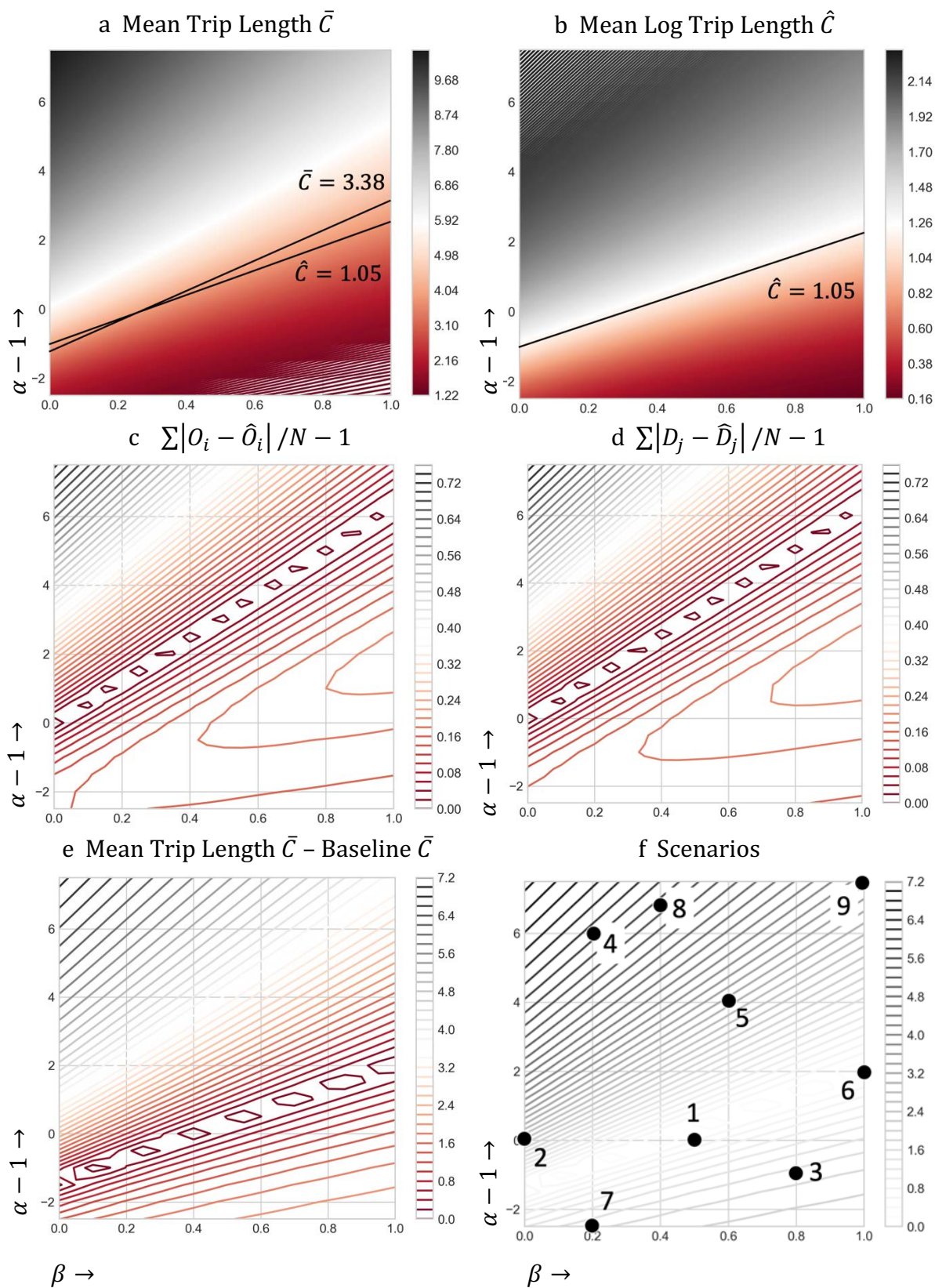

Figure 9: Representations of the Parameter Space $\propto -1\ viz\ \beta$ with Sample Scenarios

20

The Break with Space, The Death of Distance

So far both our model and the hypothetical grid city to which it has been applied have focused on how space and distance act to pull and push working populations between where they live and where they work. The strong symmetry and the focus on the geometric centre which the square grid implies act to pull activity away from the edges of the system towards the centre which most of the variations in the parameters that control the effect of distance serve to reinforce. Only when we introduce deterrence functions based the gamma, do we move populations away from their origins generating systems that begin to explode towards their peripheries. In this last section, what we will do is extend our explorations to deal with lowering the impact of space and distance on the overall system that we have already incorporated artificially through ensuring that a certain proportion of workers work from home. Our baseline for this is the observed drop in people at work to 80 percent below the usual capacity of workplace locations although we will look at other percentage changes. In this section, we pursue three variants of this release from lockdown as well as introducing diversity into the system through randomness in location and scaling to much bigger grid systems

First, we will examine the situation where we keep the lockdown at differing percentages below the normal baseline, and for each percentage level, we will look at how the system adjusts according to gravitational forces. We keep the percent below the baseline stable as the process of readjustment in location occurs for those who continue to work at their traditional workplaces. This then produces a new normal. Second, we will examine what happens when the percentage of the population in lockdown is restored step-by-step 'towards' the old normal (100 percent working traditionally) but with the distribution of work and residence adjusting throughout this process. This too is a new normal but different from the old normal and different from the situation where the numbers of persons working from home remains the same. This simulates the situation where the disruption from the baseline moves back towards the situation where no one works from home any longer. Third, we will look at how the situation restores itself to no one working from home but this time with travel behaviour based on the gamma function changing to account for persons working and living much further away from others. This is where people react to distance in a an almost opposite way to the effects of traditional distance deterrence. This provides us with new scenarios that we then proceed to diversify, first by throwing in some random noise pertaining to where people who are not locked down live and work, and then examining the long term equilibrium. We finish with growing the system to a much bigger hypothetical grid, reminiscent in scale to the way small areas are configured in London. We do not go as far as transferring our analysis to London but simply point the way to making the model more realistic. To an extent we can see all this as changing the role of space and density in cities as well as embodying Cairncross's (1997) 'death of distance' or at least its transformation in the evolution to a new normal.

In essence, the first variant is to simulate changes in the location of essential workers in terms of work and home while keeping the percentage of workers working from home constant at $1 - \lambda$. In short we let those who have not changed their working habits during the pandemic readjust to a changing urban landscape but keep those who are locked down working from home the same. We do this for different proportions in the range $0 \leq \lambda \leq 1$. We first restate the balance equations in (13) and (16) which divides workers into those who work in traditional locations and those who work from home. These are

$$\left.\begin{array}{l} \hat{O}_i = \lambda O_i + (1-\lambda)O_i \\[2mm] \hat{D}_j = \lambda D_j + (1-\lambda)O_j \end{array}\right\} \qquad . \qquad (22)$$

Note that the second term on the RHS of equations (22) is the number of people who live in origin zone i and the number of those same people who work in the same destination zone j where when these are the same $i = j$, workers do not make any trips but work from home. We then simulate the re-adjustment in locations of those traditional workers using the origin and destination terms $\hat{O}_i$ and $\hat{D}_j$ as attractors in the model that redistributes these workers. This is the usual unconstrained gravity model that can be stated as

$$\hat{T}_{ij} = \lambda K \hat{O}_i \hat{D}_j f(d_{ij}) = \lambda T \frac{\hat{O}_i \hat{D}_j f(d_{ij})}{\sum_i \sum_j \hat{O}_i \hat{D}_j f(d_{ij})} \qquad , \qquad (23)$$

where we are able to compute these changed locations for λO_i and λD_j as

$$\tilde{O}_i = \sum_j \hat{T}_{ij} \text{ and } \tilde{D}_j = \sum_i \hat{T}_{ij} \qquad . \qquad (24)$$

We can generate total new origins and destinations as

$$\left.\begin{array}{l} \hat{O}_i' = \tilde{O}_i + (1-\lambda)O_i \\[2mm] \hat{D}_j' = \tilde{D}_j + (1-\lambda)O_j \end{array}\right\} \quad \text{where} \quad \sum_i \hat{O}_i' = \sum_j \hat{D}_j' = \lambda T \quad , \qquad (25)$$

and then use these values again to redistribute those who work traditionally by substituting $\hat{O}_i'$ and $\hat{D}_j'$ for $\hat{O}_i$ and $\hat{D}_j$ respectively into equation (23) and reiterate.

The process of reiteration can continue indefinitely using the following sequence based on the unconstrained model. In indexing the model in equation (23) by time $t + 1$, we get

$$\left.\begin{array}{l} \hat{T}_{ij}(t+1) = \lambda K(t) \hat{O}_i(t) \hat{D}_j(t) f(d_{ij}) \\[2mm] \hat{O}_i(t+1) = \sum_j \hat{T}_{ij}(t+1) + (1-\lambda)O_i \\[2mm] \hat{D}_j(t+1) = \sum_i \hat{T}_{ij}(t+1) + (1-\lambda)O_j \end{array}\right\} \qquad . \qquad (26)$$

Continued substitution from the outputs of equations (26) into its inputs leads to a sequence that we consider is likely to converge as we demonstrate in the applications below on our hypothetical grid. We cannot prove that this iteration converges but we consider the strong symmetry on the grid is likely to ensure this. We can do this for all the variants in this section but first we have examined the convergence for a sequence of values in the range $0 \le \lambda \le 1$. We start all these simulations from the lockdown whose data we compute from the basic data for the hypothetical city as represented in equations (22). In fact we will show only one of the percentages locked down, not the 80% but 50% which we consider more likely as the pandemic begins to ease in the UK.
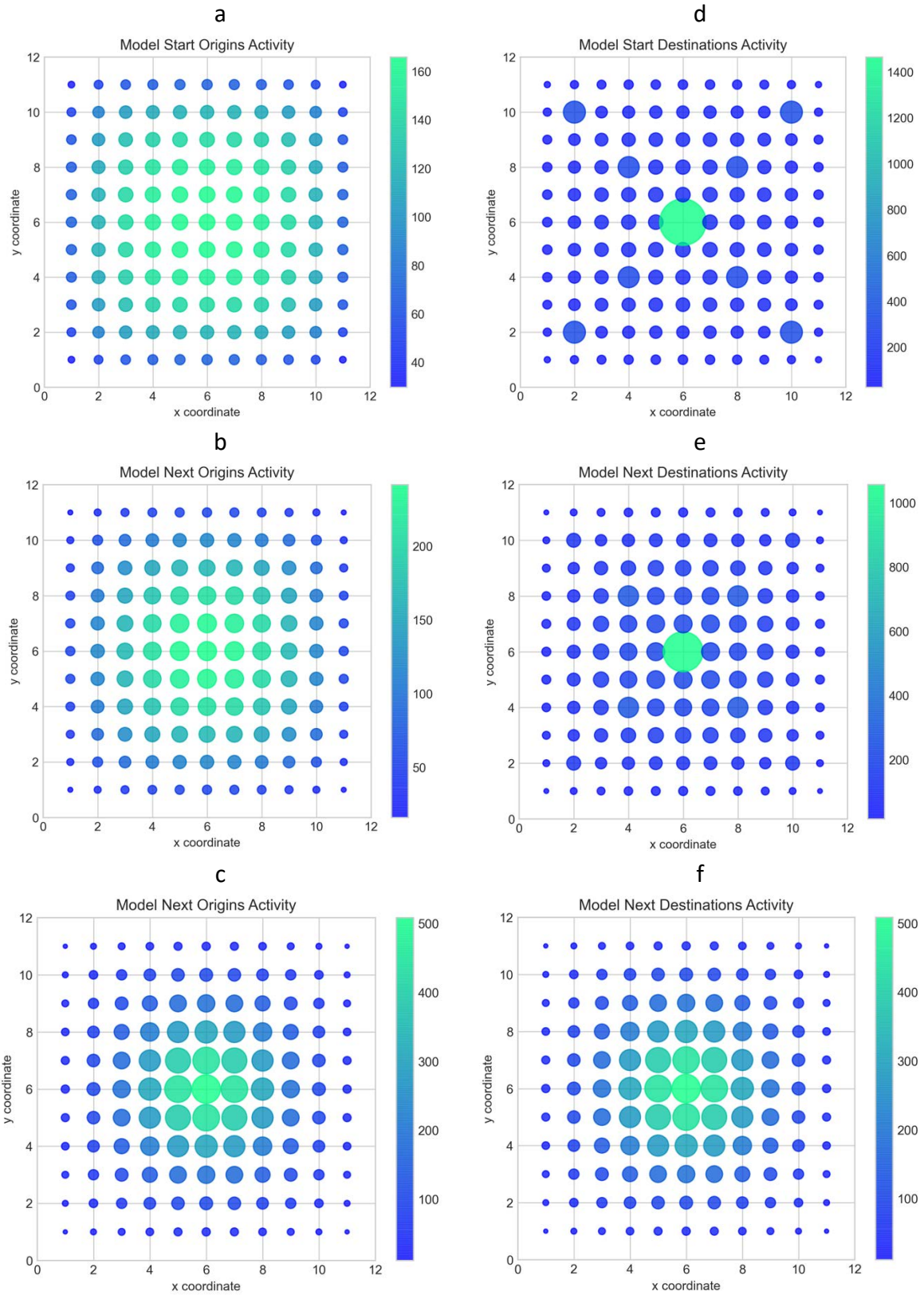
Figure 10: Transition to Long Term Equilibrium with $1 - \lambda = 0.5$ *Continuing to Work at Home*

a) Starting Origins *t=1* b) Starting Origins *t=1* c) First Origin Predictions *t=2* d) First Destination Predictions *t=2*
e) Long Term Origins *t=50* f) Long Term Destinations *t=50*

What we see when we examine this lock down is that as 50% of the activity is continually redistributed, the origin and destinations activities converge to unique patterns but that the origin and destination activity converge on each other. In this limit, it appears that the pattern of work is identical to the pattern of residence. This also seems to be the case for any value of $1 - \lambda$ but in Figure 10, we only show that for $1 - \lambda = 0.5$. In fact we show a lower value $1 - \lambda = 0.2$ and a higher value $1 - \lambda = 0.8$ in the Appendix where we include a lot of the more routine visualisations that need to be understood and scanned but are merely supportive of the continuing argument. In Figure 10, the ultimate pattern seems plausible given the fact that when only 50% remain working from home, the rather flat but centralised distribution of these workers remains stable while those working traditionally are able to respond to the attractions of those who work from home as well as the distribution of their own workplaces which are highly monocentric but also polynucleated. This in fact is a feature that will continue to dominate all these examples.

Our second case is based on a return to normality with the numbers of people working from home as 10% ($\lambda = 0.1$) through to everyone working traditionally (with none at home). However as this transition takes place, the working population at workplaces (destinations) and residences (origins) continually adjusts to the changing landscape. We simulate this using the unconstrained gravity model but with the temporal index now linked to the level of home working. We write the model based on equation (26) as

$$
\left.
\begin{aligned}
\hat{T}_{ij}(\lambda_{t+1}) &= \lambda K(\lambda_{t+1})\hat{O}_i(\lambda_t)\hat{D}_j(\lambda_t)f(d_{ij}) \\[2mm]
\hat{O}_i(\lambda_{t+1}) &= \sum_j \hat{T}_{ij}(\lambda_{t+1}) + (1 - \lambda_{t+1})O_i \\[2mm]
\hat{D}_j(\lambda_{t+1}) &= \sum_i \hat{T}_{ij}(\lambda_{t+1}) + (1 - \lambda_{t+1})O_j
\end{aligned}
\right\} \qquad , \qquad (27)
$$

where λ_{t+1} is the proportion of population locked down and working from home. The transition from $0.1 \leq \lambda_{t+1} \leq 1.0$ can be as smooth as required and from this it is easy to make a movie showing how the centralising and decentralising forces act themselves out.

In fact in the Appendix, we provide a glimpse of the key frames of such a movie at steps of 0.1 showing how the population moves back to full time working while at the same time centralising and converging on a longer term equilibrium which forces residential and workplace locations together. The solutions that we show in Figure 11 are theoretical possibilities but never likely to be manifest in this form. This however does provide a sense in which there can never be a transition back to normality for the way people will react is likely to be different from the way they have done in the past prior to the pandemic with respect to location. In fact, the 10-fold transition from $0.1 \leq \lambda \leq 1.0$ in steps of 0.1, along with the responses to the changed landscape of origins and destinations propel the city into a relatively concentrated form quite quickly, seemingly at a faster rate than when the percentage of persons working from home remains constant with rates of more than about 25%. The last substantive change we will make is to introduce the gamma deterrence function that enables workers to locate at much further distances from one another than we currently observe. We illustrate this in the 9 scenarios explored above in the analysis where we replaced the deterrence function with one combining power and exponential components into a form that balances attraction for living at greater distances away with the benefits of living nearer to any place.
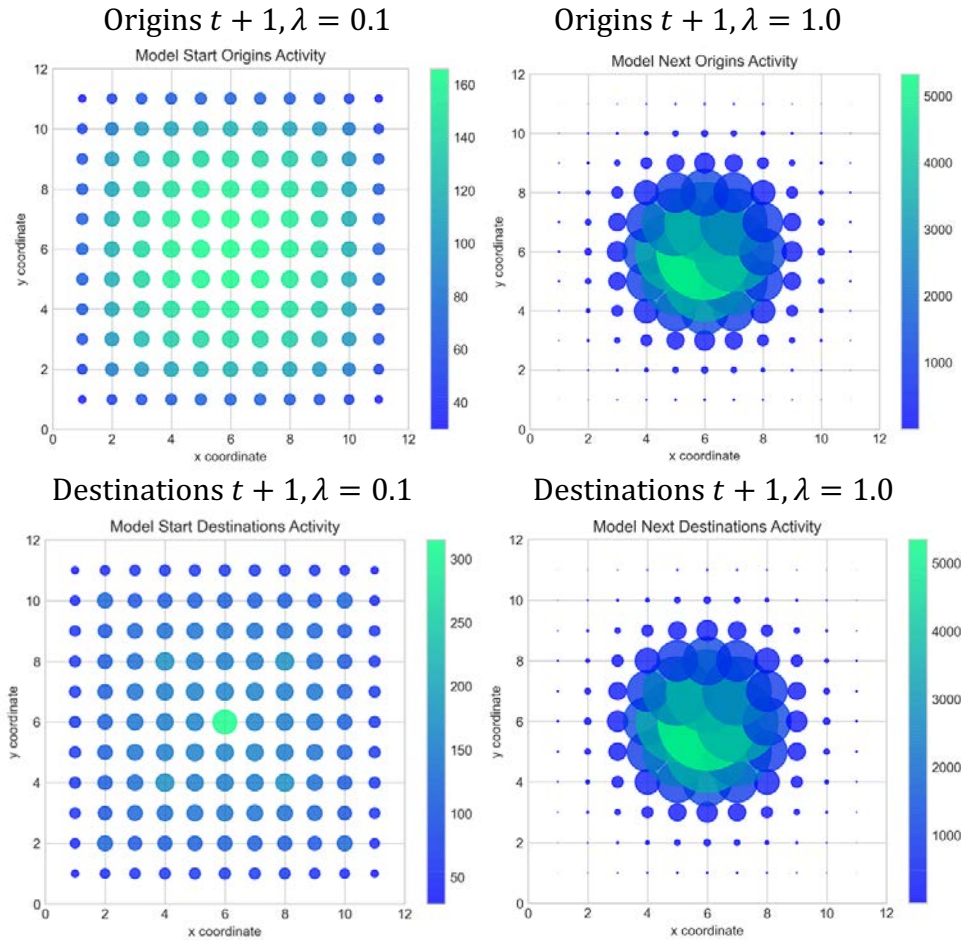
Figure 11: Transitions from Lockdown with 10% Working from Home
Through to 100% Traditional Working

These functions are shown in Figures 7 to 9 and in this section we will choose one of these that redistributes workers where the attractiveness of location increases the further away from the origin to a peak after which it subsides. This function is $d_{ij}^6 \exp(-0.2d_{ij})$ which quickly redistributes the percentage of workers working traditionally in terms of where they live and work and as in the other variants in this section, we run the model in equations (26) but now with the new function. This generates the following sequence where the density of activity at the outset has 10% of the population working at home, and redistributes itself to move towards the edge of the system. By the time everyone is back at work, the activity is largely located at the furthest distances from the centre of the grid, that is at the four corners of the square system.

We show this in Figure 12 where it is clear that there are many ways in which we can redistribute activities reflecting the balance between centralisation and decentralisation combining different deterrence functions with ways of locking down the population and seeding activities in suburban areas. This balance of inward and outward forces also reveals some very deep issues in terms of this kind of analysis. It is quite obvious that the development of a hypothetical grid system with all its focus on its most accessible point being its centre and its least accessible the four corners of the square grid provide limits when we come to develop this analysis for real cities and when we scale up our grid to truly huge dimensions. It might be argued that all that this effort has done is to reveal the

major problems of space, density, deterrence and boundary definition for problems involving how we travel and locate in cities but in doing so, we focus attention on the geometry of cities which has barely been explored to date other than in the most superficial terms. This is mainly due to the fact that we only now have the technology to begin to search over many alternative forms, to explore solution spaces where most solutions are infeasible or outrageous, and to begin to search for the urban forms that are most likely to emerge under certain plausible conditions. This then is a challenge for future research.
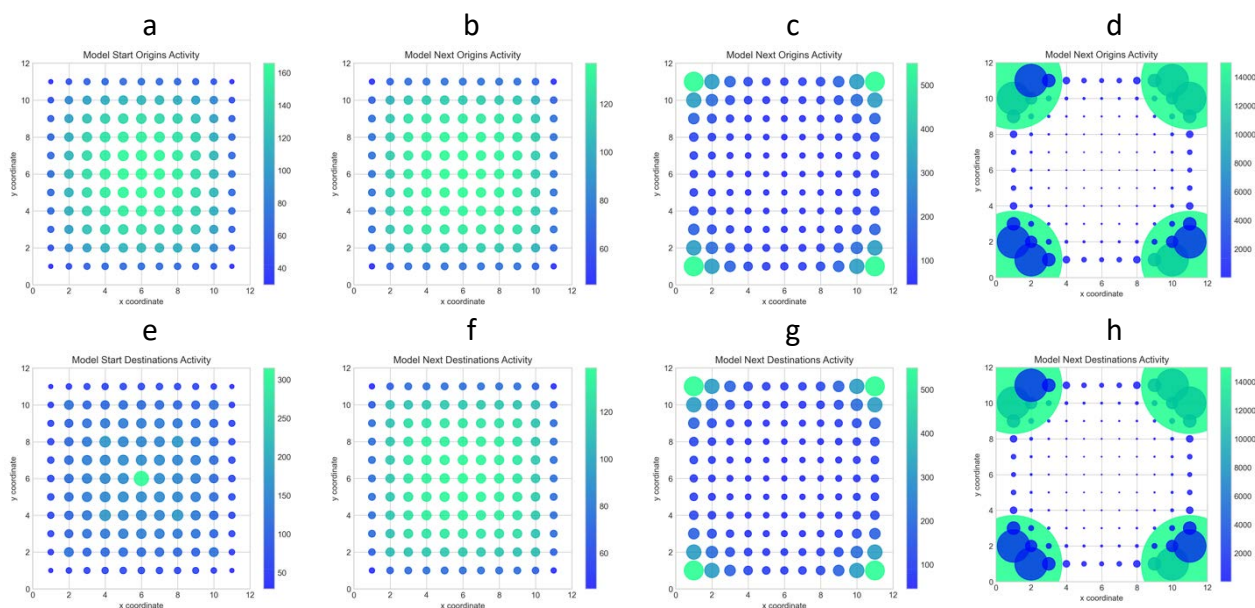
Figure 12: A Switch in Travel Behaviour: Scenario 4: α-1=6, β=0.2, using the Gamma Function $\sim d_{ij}^{6} \exp(-0.2 d_{ij})$

Origin Activities a) t=1 b) t=2 c) t=5 d) t=10: Destination Activities e) t=1 f) t=2 g) t=5 h) t=10

The last thing we will do is to introduce a degree of randomness into this picture just as we did in an earlier section where we modified the origins and destinations using a fairly large random switch with an average of $\pm 25\%$ differences from the basic input data. We do the same for the model in equations (26) where we also use the gamma function and the release from lockdown. This is alongside the introduction of a degree of randomness at each iteration of the release from lockdown which takes place over 10 time periods from $0.1 \leq \lambda_{t+1} \leq 1.0$ in steps of 0.1. The most surprising feature of the outcomes from this model involve the convergence to what appears a relatively stable solution for both origin and destination distributions while it appears that not only do these distributions converge but they also converge towards each other in terms of the similarity of activity levels at the same locations. All these simulations are shown in Figure 13. We cannot definitely demonstrate this but in the move to realism that we will mark out in our final section, it appears that we should be able to generate more realistic solutions, largely through introducing much more uneven surfaces to the simulation. In short, to get more realistic simulations, we need much greater diversity and heterogeneity in the distributions of origins and destinations as well as in the regularity or otherwise of the grid.
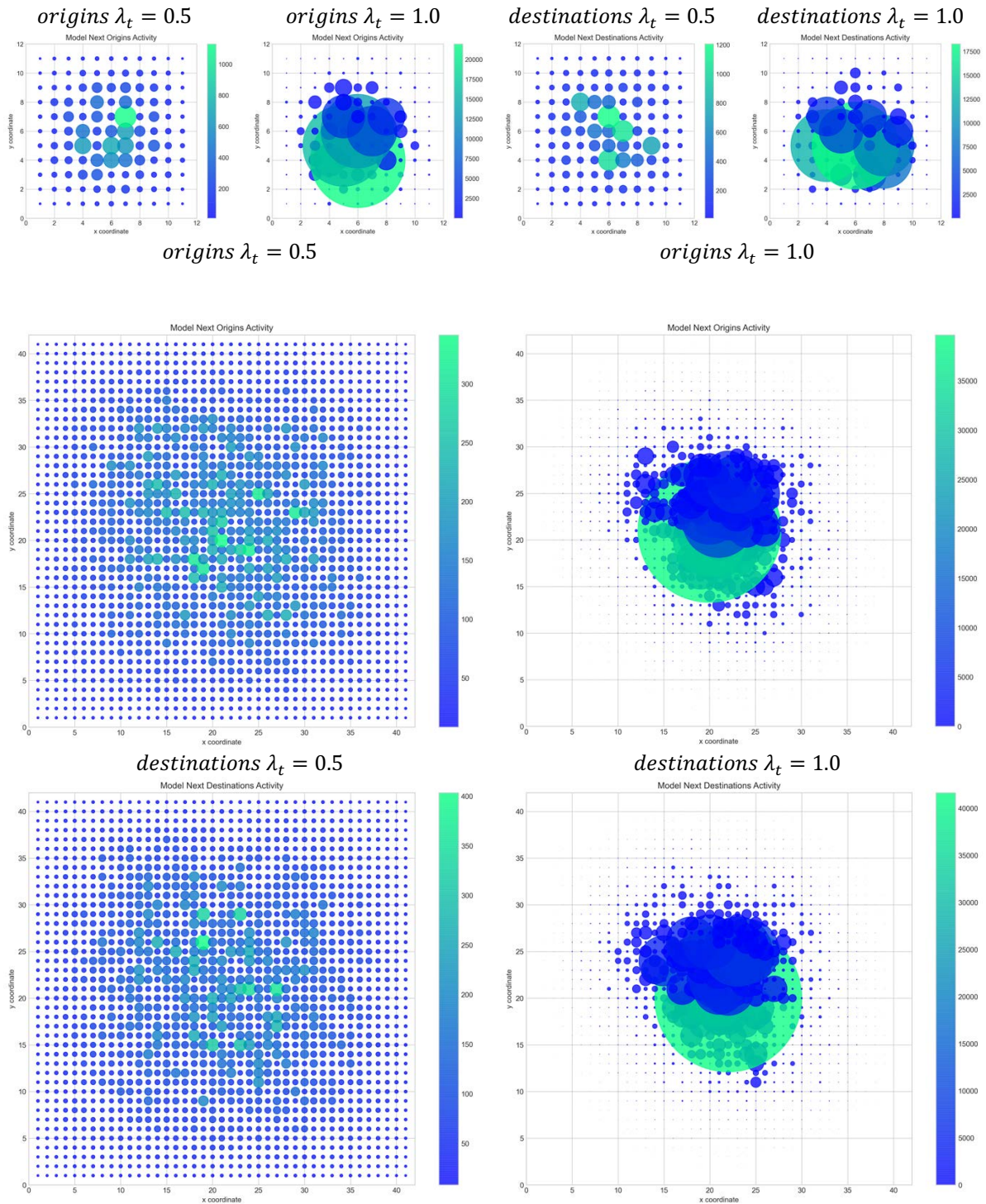
Figure 13: Introducing Randomness and Scaling Up the System
from 11x11=121 Zones to 41x41=1681 Zones

Towards Realism

The hypothetical city and its model introduced in this paper is a far step from the cities that compose our material world. But in a situation where we are 'forced to live' in an artificial world of lockdown where every locational pattern and set of interrelationships

that define a city have been dramatically disrupted, one way of approaching the problem of how the future city will evolve after the pandemic ends is by developing an abstract model that we can experiment upon. No one can pretend that this is a model of a real city but like any model, we believe it contains the kernel of what makes a city function with respect to the flows and forces that determine where people live and work while at the same time, encapsulating the history of large cities that are built up through history, layer upon layer at a time around the traditional core with the city growing every bigger as it expands outwards.

The push and pull forces that determine movement and location were first articulated during the early industrial revolution but they have become more convoluted with time. In the middle years of the last century, one of the great intellectual leaders of planning, Catherine Bauer Wurster (1963) wrote an essay entitled 'The Form and Structure of the Future Urban Complex' in which she argued that the form of the future city would reflect the age old tension between these forces, arguing that this balance is never simple and there are contradictory trends in both directions. This is what we have seen in this paper, the difficulty of working out what determines location and movement with respect to the balance between the artificiality of lockdown, the penchant for movement to lower density living on the edge of the city, the quest to social distance at different scales and the decline in working at the centre and any of the denser hubs that make up the traditional city. We have collapsed all of these forces into distance deterrence functions combined with different degrees of lockdown and its release but also with the ability of workers who are not locked down to respond to the new landscape of location that emerges as workers continually reconsider their decisions as to where to live and work.

The hypothetical city we have built and modelled using standard spatial interaction functions has provided us with an environment in which to experiment with future forms that are no more extreme than the current artificiality of lockdown. This in itself is something that would not emerge without radical changes in locational behaviour and is assumed to be temporary until the pandemic which caused it is controlled. We do not know when this will be – we assume sometime during the next year – but we have little idea as to how much of the change that has already happened will become incorporated in the fabric of the post-pandemic city. We have attempted to simulate this using a variable deterrence function that can encapsulate everything from extreme centralisation to extreme decentralisation but how far the population will adjust in this way while at the same time moving to more attractive locations remains one of the great open questions that this paper pinpoints. The answers that we have given to this are speculations based on our simulations and simply provide a forum for informed discussion: these are not predictions. Just as the pandemic was entirely unpredictable as have been our responses to it, so too will be the post-pandemic future when it comes to where we will live and work and how we will move (Batty, 2018).

The way we have simulated the return to a new normal in this paper is based on assuming that once workers are no longer constrained to work at home, they will begin to function by responding to changed patterns of location that they themselves will continue to change. The forces that make these locations change are contained in behaviours that are simulated using deterrence functions where we introduce plausible changes from the old normal. In short, we examine the longer term equilibrium states that are predicted by the model as workers continually respond to the new surfaces of locational attractions that

emerge long after the lockdown is lifted. From this discussion, what emerges in this model is that the forces of centralisation are so strong in our hypothetical grid city that under most of the scenarios that we have examined here, the pattern of centrality that we define as the old normal is reinforced as the lockdown is released with the long term equilibria based on extreme concentrations at the core. This implies that far from the city exploding and people moving to the distant suburbs, people will return to the city. Only when we change behaviour radically to incorporate a penchant for living at great distances away from work and other residential locations do we see cities which explode in their peripheries. Implosion in fact appears to be the more likely future than explosion. However, much of this depends on whether or not we will change our travel behaviour and a radically new normal will only emerge if such change occurs.

To make our model more realistic, we need to introduce much greater diversity into the framework. We need to enable symmetry to be broken and we have shown how hard this is requiring quite radical changes in interaction and location. We probably need to develop a more controlled and extensive exploration of possible futures using the hypothetical city but to really engage in more realistic speculation, we need to move this to a real city. Real cities have a much more heterogeneous patterns of land use, they have many more holes in their fabric, and they depend to a large extent on physical topographies that have determined and continue to influence their historic evolution. We also need to break symmetry using actual transport and other networks and to do this, we need to develop these ideas for relatively well-formed mono-centric cities like London. Figure 13e-h shows a picture of origins and destinations for a grid similar in size to London and its outer metropolitan area based on its usual geographic zoning as we have used in our land use transportation models of the city (Batty et al., 2013). To move our ideas to this geometry would be a natural extension of the ideas developed here and in future work we will attempt this. However we consider it important to retain the blue-skies thinking that we have introduced here in to-ing and fro-ing between the hypothetical and the real for only in this way can we explore the limits that are placed on our future cities.

References

Apple (2021) *Mobility Trends Reports*, https://covid19.apple.com/mobility

Batty, M. (2018) *Inventing Future Cities*, The MIT Press, Cambridge, MA.

Batty, M. (2020b) Social Distancing at Scale, *Environment and Planning B: Urban Analytics and City Science*, **47**(9), 1533–1536.

Batty, M. (2020a) The Coronavirus Crisis: What Will the Post-Pandemic City Look Like? *Environment and Planning B: Urban Analytics and City Science*, **47**(4), 547–552.

Batty, M., and March, L. (1976) The Method of Residues in Urban Modelling, *Environment and Planning A*, **8**, 189-214.

Batty, M., Vargas, C., Smith, D., Serras, J., Reades, J., and Johansson, A. (2013) SIMULACRA: Fast Land-Use–Transportation Models for the Rapid Assessment of Urban Futures, *Environment and Planning B*, **40**, 987 – 1002.

Cochrane, R. A. (1975) A Possible Economic Basis for the Gravity Model, *Journal of Transport Economics and Policy*, 9, 34-49.

Coleman, J. S. (1964) *Introduction to Mathematical Sociology*, The Free Press, Glencoe, NY.

Couclelis, H. (2021) Conceptualizing the City of the Information Age, In Shi, W., Goodchild, M., Batty, M., Kwan, M. P., and Zhang, A. (Editors) *Urban Informatics*, Springer, Berlin and New York, forthcoming, doi.org/10.1007/978-981-15-8983-6_2

Farquharson, C. Rasul, I., and Sibieta, L. (2020) *Key Workers: Key Facts and Questions*, Institute of Fiscal Studies, London, accessed 31/10/20, available at https://www.ifs.org.uk/publications/14763

Florida, R., Rodríguez-Pose, A., and Storper, M. (2020) Cities in a Post-COVID World, *Papers in Evolutionary Economic Geography, No. 20.41*, Utrecht University, The Netherlands: Department of Geography, at http://econ.geo.uu.nl/peeg/peeg2041.pdf

Google (2021) *Community Mobility Reports*, https://www.google.com/covid19/mobility/

Nugraha, A. T., Waterson, B. J., Blainey, S. P., and Nash, F. J. (2020) On the Consistency of Urban Cellular Automata Models based on Hexagonal and Square Cells, *Environment and Planning B: Urban Analytics and City Science.* https://doi.org/10.1177/2399808319898501

Sui, D. Z. (2004) Tobler's First Law of Geography: A Big Idea for a Small World? *Annals of the Association of American Geographers*, 94(2), 269–277.

Tanner, J. C. (1961) *Factors Affecting the Amount of Travel*, Technical Paper 5, Road Research Laboratory, London.

Tobler, W. (1970) A Computer Movie Simulating Urban Growth in the Detroit Region, *Economic Geography*, **46**, 234–40.

Tobler ,W. (1976) Spatial Interaction Patterns, *Journal of Environmental Studies*, **6**, 271-301.

Wurster, C. B. (1963) The Form and Structure of the Future Urban Complex. In L. Wingo, Jr. (Editor) *Cities and Space: The Future Use of Urban Land*, Johns Hopkins Press, Baltimore, MD, 73-102.

Zhu, R., et al. 14 co-authors (2021) *The effects of different travel modes on COVID-19 transmission in global cities*, Key Laboratory of Virtual Geographic Environments, Nanjing Normal University, Nanjing, PRC.

Appendix: Supplementary Material

Interpreting The Grid Maps

The graphics in this paper have been produced using Matplotlib in Python and it is important to make clear the way they should be read. The hypothetical square grid is composed of $n \times n$ square cells whose centroids represent the locations which we associate with the volumes of activity – the working population at their residences or origins O_i and the same population at their workplaces or destinations D_j. All our maps of this grid city plot the size of activity in proportion to its observed or predicted volumes as a circle at the point location. If and when the circles begin to overlap, then a transparency criterion is invoked and it is possible for the reader to intuitively understand the underlying trends although the more the reader is familiar with the data and the simulations, the easier it is to interpret these maps. The size of each point is based on the area of the appropriate circle. If the activity size is $O_i = 100$ units, for example, the area of the circle is proportional to $\sim \sqrt{O_i} \sim 10$. The colour is also related linearly to size but the range of values varies for each map so that the maximum contrast over the range of values is employed.

The 9 Scenario Plots for Different Combinations of the Gamma Function Parameters
#### Scenario 1: $\alpha - 1 = 0$, $\beta = 0.5$, $\bar{C} = 2.95$, $\hat{C} = 0.91$
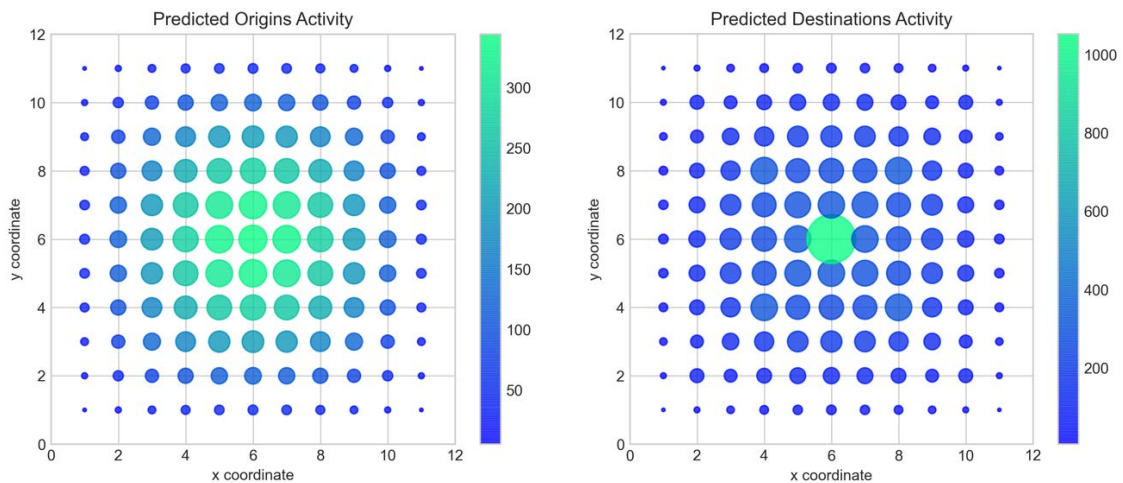
Scenario 2: $\alpha - 1 = 0$, $\beta = 0.0$, $\bar{C} = 5.43$, $\hat{C} = 1.53$
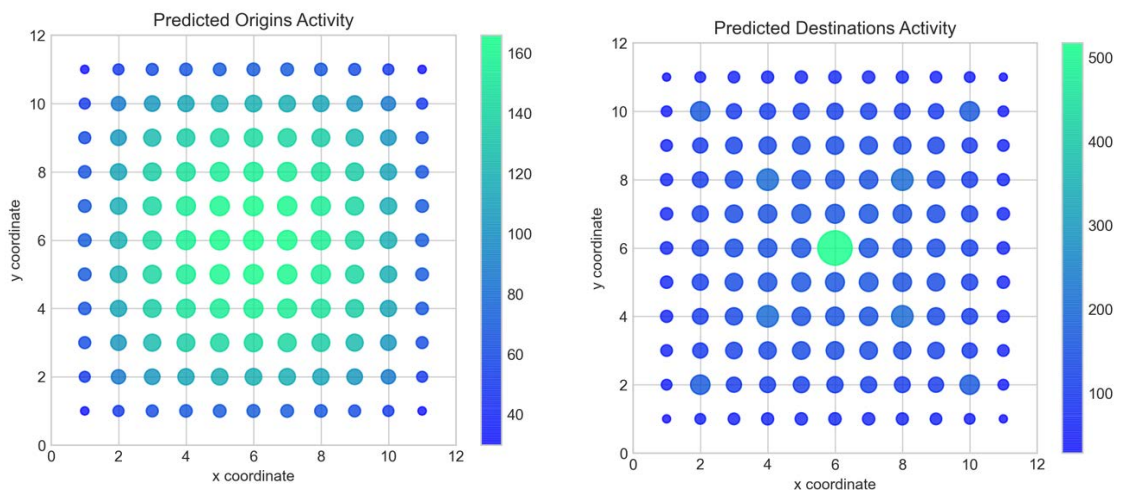
Scenario 3: $\alpha - 1 = -1,\ \beta = 0.8,\ \bar{C} = 1.71,\ \hat{C} = 0.42$
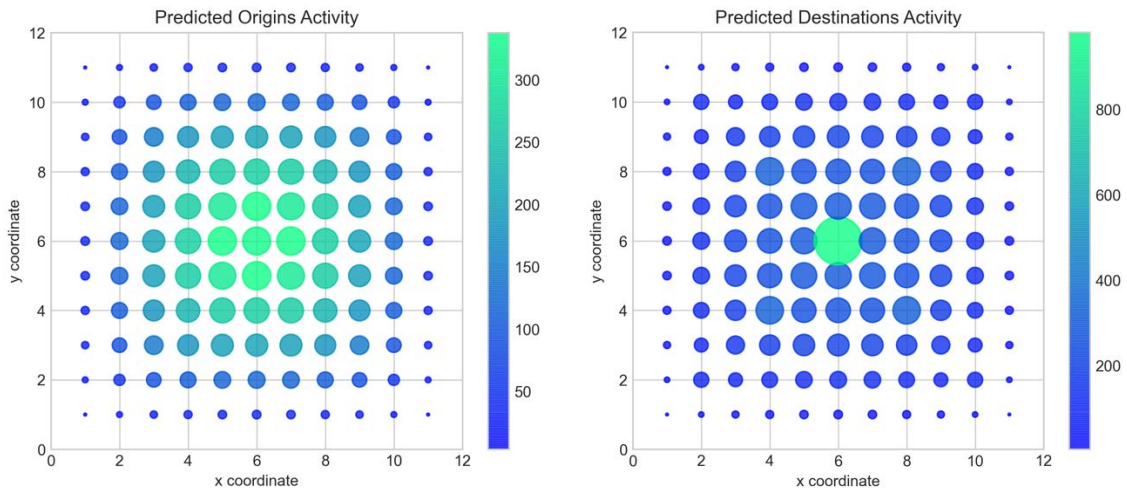
Scenario 4: $\alpha - 1 = 6,\ \beta = 0.2,\ \bar{C} = 8.86,\ \hat{C} = 2.16$
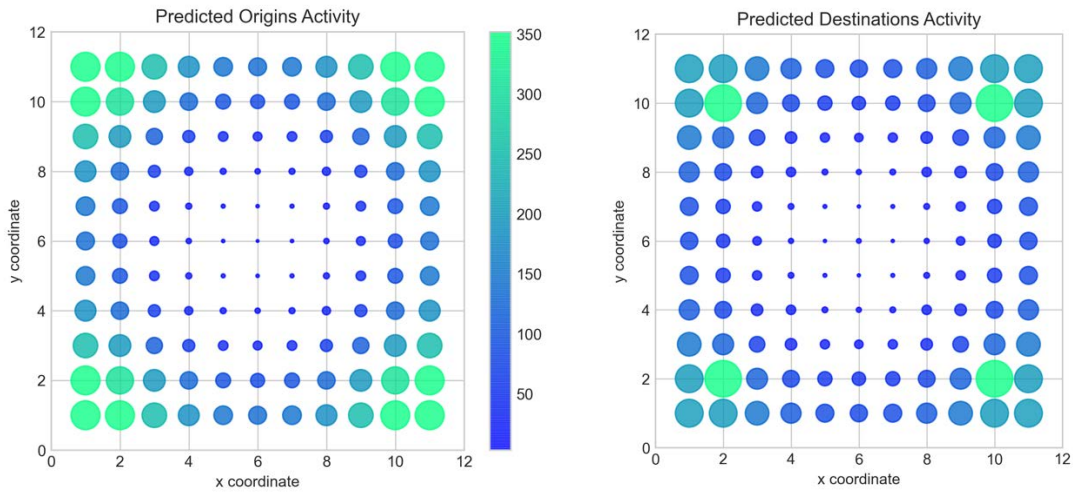
Scenario 5: $\alpha - 1 = 4,\ \beta = 0.6,\ \bar{C} = 6.17,\ \hat{C} = 1.76$
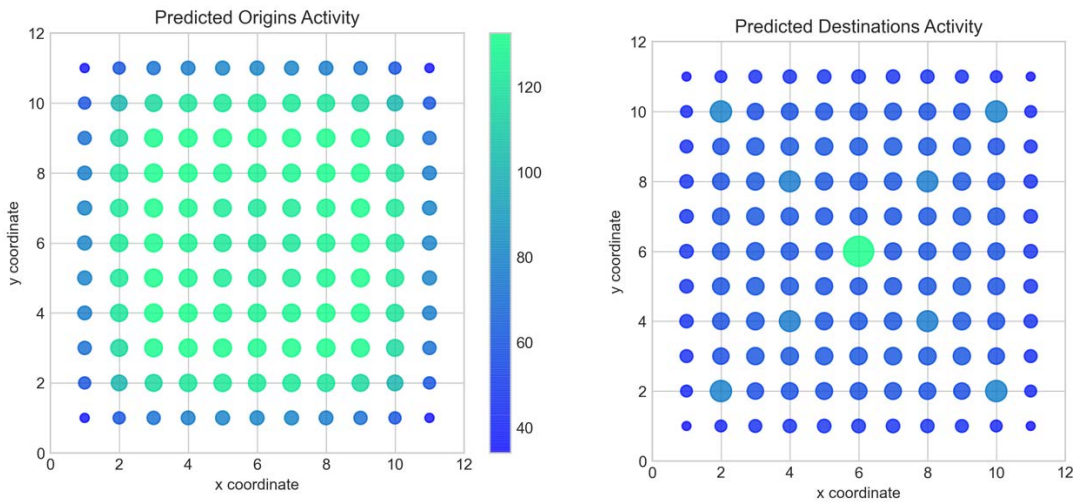
Scenario 6: $\alpha - 1 = 2$, $\beta = 1.0$, $\bar{C} = 3.33$, $\hat{C} = 1.08$
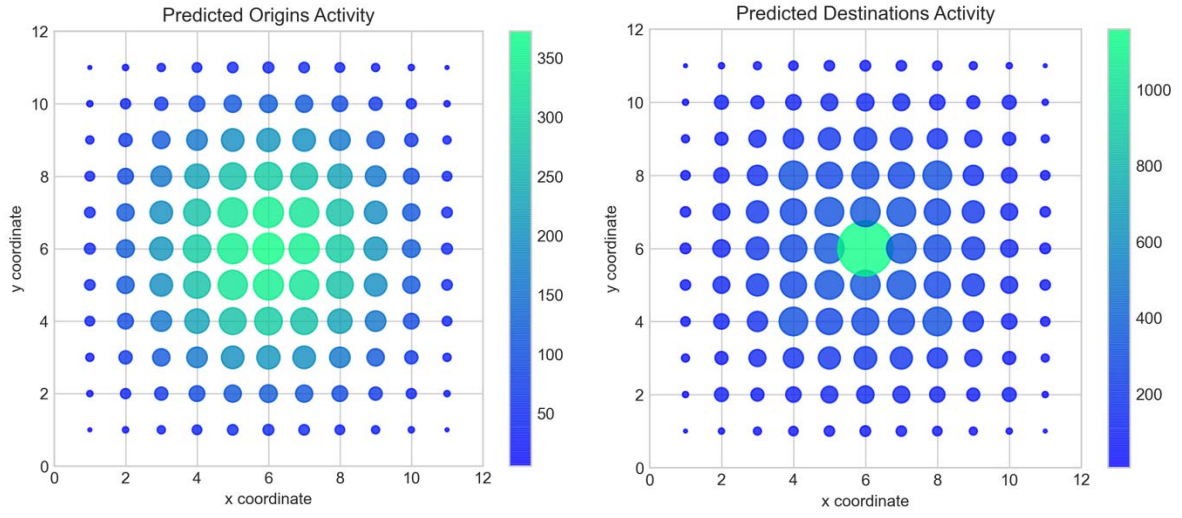
Scenario 7: $\alpha - 1 = -2.5$, $\beta = 0.2$, $\bar{C} = 1.65$, $\hat{C} = 0.37$
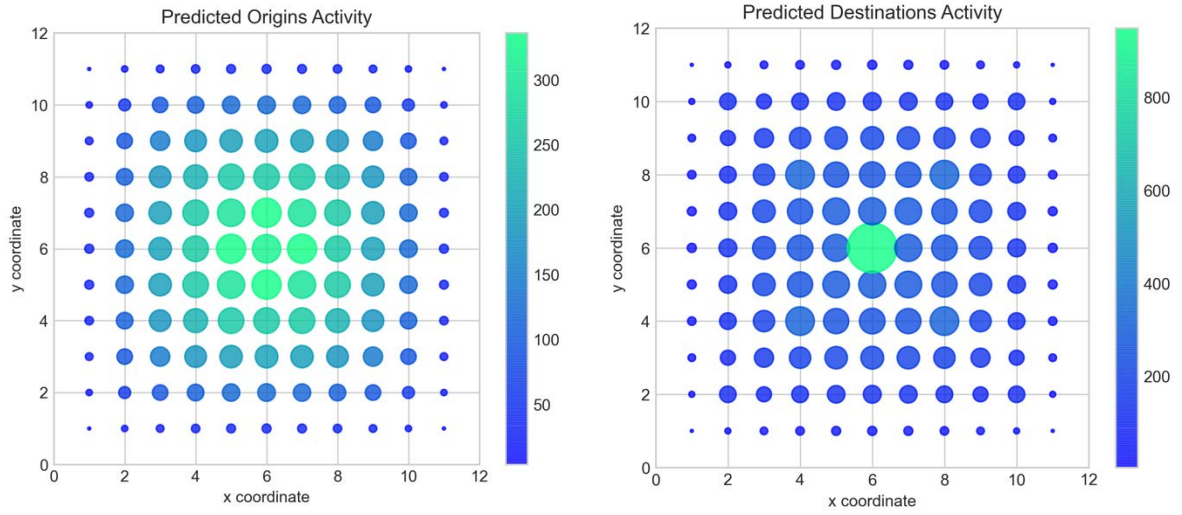
Scenario 8: $\alpha - 1 = 7$, $\beta = 0.4$, $\bar{C} = 8.59$, $\hat{C} = 2.12$
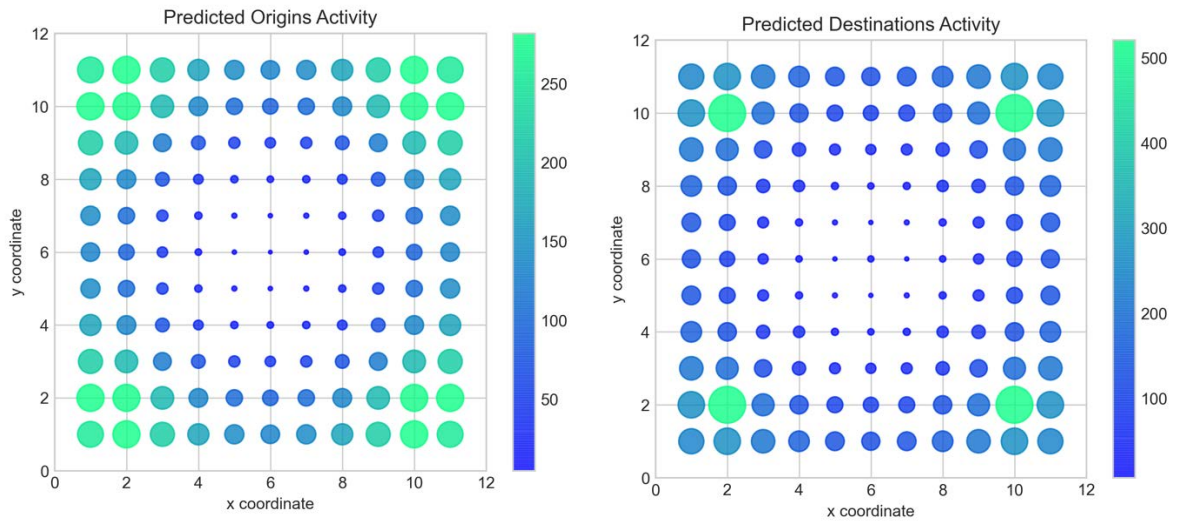
Scenario 9: $\alpha - 1 = 7, \ \beta = 1.0 , \ \bar{C} = 6.78, \ \hat{C} = 1.88$
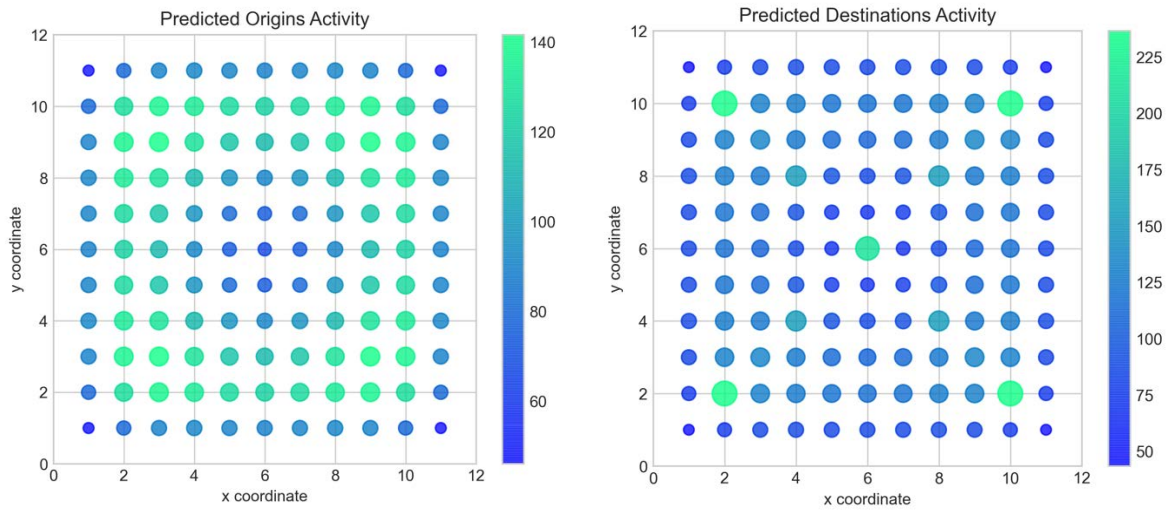
Figure A1: Predicted Origins and Destinations From the Baseline Lockdown

Key Frames from the Release of the Lockdown Based on Increasing λ By Steps of 0.1

You could almost cut out the frames and make a flick book from these collages but this gives some idea of the need to experiment with such systems as they are running on the desktop for only then can the essence of this experimental manipulation be appreciated.

Origins
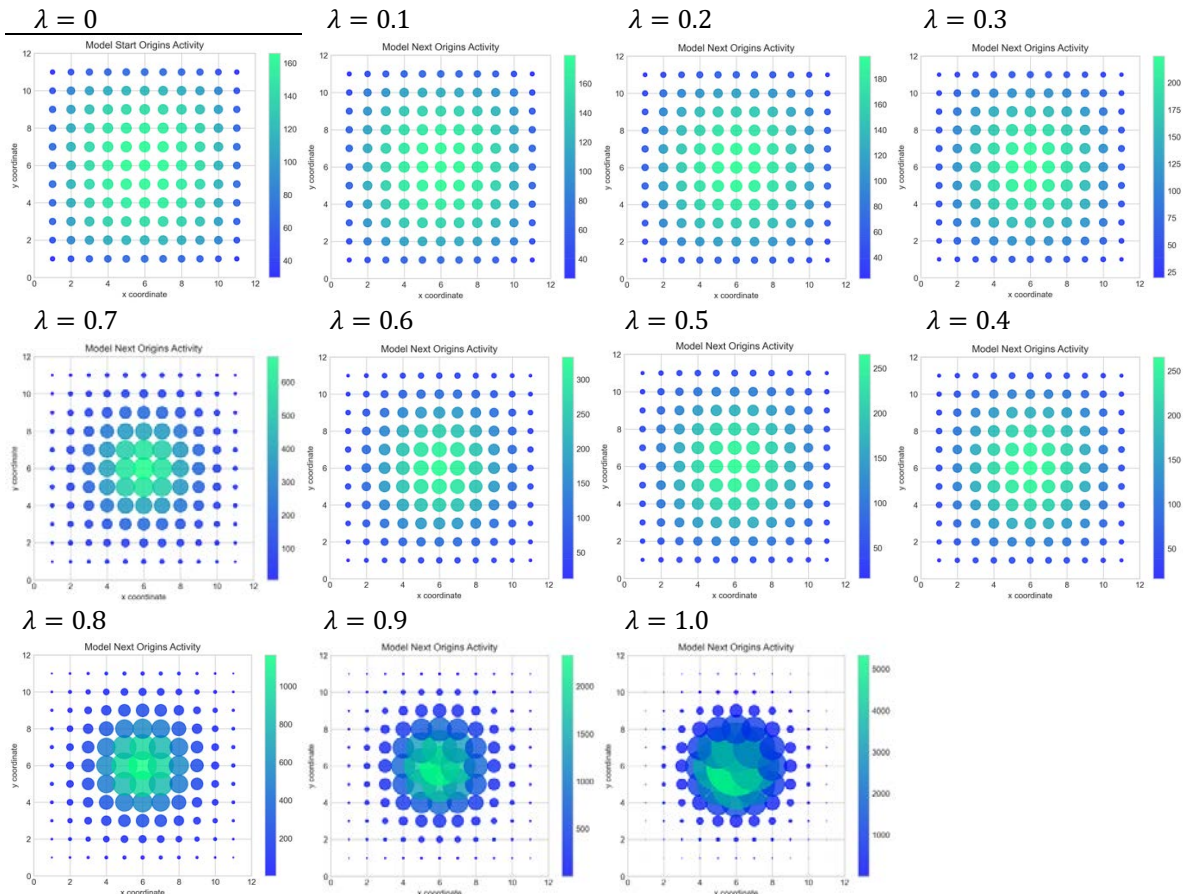
Destinations
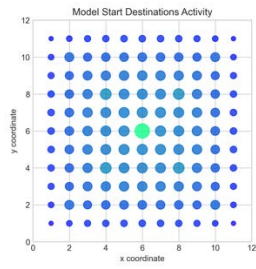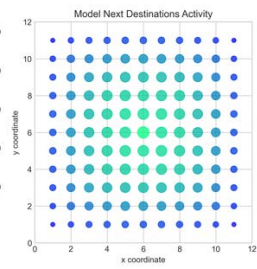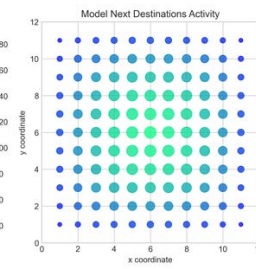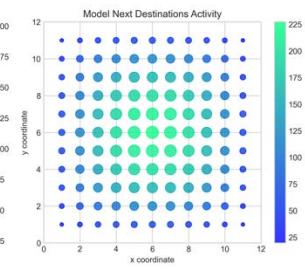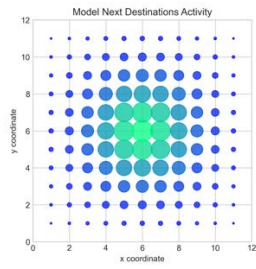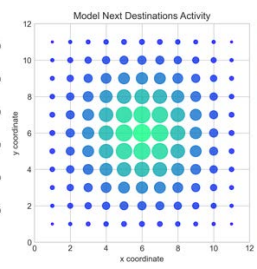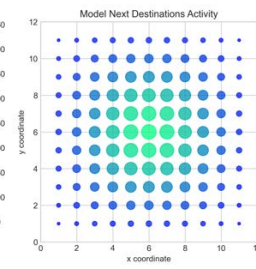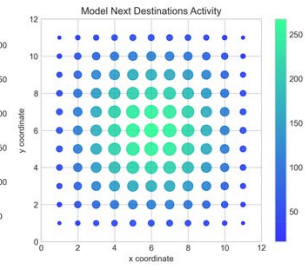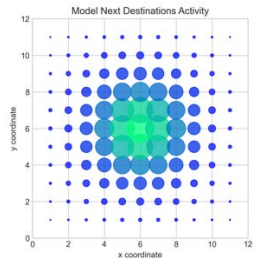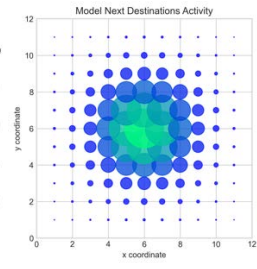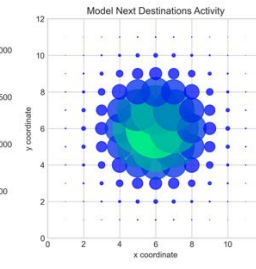
Figure A2: Transitions from Complete Lockdown Back to the Old Normal